Palaeoenvironmental reconstruction by means of palynofacies and lithofacies analyses: an example from the Upper Triassic subsurface succession of the Hyblean Plateau Petroleum System (SE Sicily, Italy)

Simonetta Cirilli [a], Giulia Panfili [a], Nicoletta Buratti [b], Alfredo Frixa [c]

S. Cirilli: simonetta.cirilli@unipg.it;

[a] Department of Physics and Geology, University of Perugia, Via Pascoli, 06123 Perugia, Italy.

G. Panfili: giupanfi@tiscali.it

[a] Department of Physics and Geology, University of Perugia, Via Pascoli, 06123 Perugia, Italy.

N. Buratti: nicoletta.buratti@total.com

[b] Total SA, CSTJF - Avenue Larribau, 64018 Pau Cedex France

A. Frixa: alfredo.frixa@eni.com

[c] Eni SpA Upstream and Technical Services Via Emilia 1, San Donato Milanese (Milano, Italy)

Corresponding author: simonetta.cirilli@unipg.it

Abstract

A combined palynofacies and lithofacies analysis was carried out on two borehole successions (Streppenosa 1 and Bimmisca 1) from the Hyblean Plateau Petroleum System (SE Sicily, Italy). It was found that both the wells penetrated the most important source and seal rocks of the Sicilian region (Noto and Streppenosa formations), previously assigned to the Late Triassic-Early Jurassic, deposited within a carbonate platform-basin system. Based on new palynological data, the organic rich succession (Noto Formation and Upper Streppenosa Member) can now be entirely assigned to the

Rhaetian, thus constraining its deposition to a time interval characterized by increasing global humidity and seasonality. The integrated palynofacies and lithofacies data enabled characteri- zation of the timing of the drowning phases of the carbonate platform-basin system as being controlled by rela- tive sea level changes mostly triggered by the Triassic extensional tectonic activity. During the first phase of the relative sea-level rise, clayey and organic-rich sediments were deposited only in the deepest portion of the basin. As the sea level continued to rise, the entire system drowned completely and suboxic-anoxic basinal sediments were deposited across the whole Hyblean region, onlapping the shallow-water facies. In the meantime increasing global humidity contributed to an increased freshwater input in the marine depositional system as documented by the presence of fern spores and clay. It caused water stratification and subsequent anoxia at marine basins, fa- voring the preservation of sedimentary organic matter. This atmospheric change could be related to the degassing of the Central Atlantic Magmatic Province.

Key words: palynofacies; palynostratigraphy; platform-basin system; Late Triassic; Sicily (Italy)

1. Introduction

The temporal and spatial distribution of Phanerozoic organic rich sediments relates to a combination of variables: organic productivity, appropriate sedimentation rates and organic matter preservation (Tyson, 2001, 2005; Katz, 2005; Trabucho-Alexandre et al., 2012). Organic carbon rich sediments have been commonly attributed to widespread ocean anoxia and to associated water column stratification that isolates the marine bottoms from the oxygen mixed zone (Tyson and Pearson, 1991; Wignall and Newton, 2001; Pancost et al., 2004; Harris, 2005; Meyer and Kump, 2008). Other theories suggest that a combination of high primary productivity and low sedimentation rate promotes the accumulation of large amounts of organic matter due to a relatively low degree of dilution by siliciclastics and skeletal debris (Lallier-Vergès et al., 1995; Perkins et al., 2008). During the Late

Triassic – Early Jurassic times in the western Tethys realm, deposition of organic rich clay and marly successions seems to coincide with a climate warming and an increasing rainfall and runoff (Korte et al., 2009; Bonis et al., 2010; Haas et al., 2010, 2012; Michalík et al., 2010; Berra, 2012). This has been interpreted as a consequence of an intense monsoonal activity (Parrish, 1993; Satterley, 1996; Sellwood and Valdes, 2007; Bonis and Kürschner, 2012). In addition, the onset of igneous and volcanic activity within the Central Atlantic Magmatic Province (CAMP), is generally believed to have strongly influenced the climate change by releasing of volcanic gases (mainly CO_2 and SO_2) into the ocean–atmosphere system (Marzoli et al. 2004; Cirilli et al., 2009; van de Schootbrugge et al., 2009; Lucas et al., 2011; Ruhl et al., 2011; Schaller et al., 2011; Pálfy and Zajzon, 2012; Vajda et al., 2013; Bond and Wignall, 2014; Lindström, 2016; Davies et al., 2017; Lindström et al., 2017b). Consequently, the end-Triassic mass exctintion (ETE) has been attributed to the huge amount of greenhouse-gas emissions in the atmosphere and in the ocean waters and associated to the ≈3-6% negative carbon isotope excursion, recorded in both terrestrial and marine environments (Schoene et al., 2010; Whiteside et al., 2010; Ruhl et al., 2011; Dal Corso et al., 2014; Lindström, 2016; Lindström et al., 2017b). Recent high-precision U-Pb ages from CAMP mafic intrusive units (Davies et al., 2017) and large scale correlations based on a set of integrated biotic, geochemical and radiometric data (Lindström et al., 2017b), document that magmatic activity started about 100 Kyr before the earlier known eruptions, providing evidence of the causal relation between CAMP and ETE. The resulting increase of fresh water supply and nutrient input in the marine environments, via river runoff, leaded to water density stratification and increased primary productivity that drove the organic matter accumulation and preservation at the anoxic marine bottoms.

The overall aim of this study is to provide new insights into the factors triggering the accumulation and preservation of organic matter within a given paleoclimatic and paleogeographic scenario related to the well-known source and seal rocks of the Hyblean Petroleum System, in south eastern Sicily

(Italy). We combined palynofacies and lithofacies analyses of two on-shore wells from Sicily in order to interpret the paleoenvironmental and paleoclimatic conditions and the input of or- ganic matter preserved in the sediments. The data provided in this paper complement and integrate those presented by Cirilli et al. (2015) regarding another on-shore well (Pachino 4) drilled in the same area.

2. Geological setting

In the last few decades, Eni Upstream and Technical Services have carried out many geological studies, in southeastern Sicily on-shore and off-shore, following exploration activity (Fig. 1) (Frixa et al., 2000; Trincianti et al., 2015 for references). The studied wells are located in the south east of Sicily (Hyblean Plateau) which is characterized by an over 5 km thick Triassic-Neogene sequence, lying above a 20–25 km thick sequence with African affinity and acting as a foreland basin during Neogene Alpine orogenesis (Patacca et al., 1979; Yellin-Dror et al., 1997; Catalano et al., 2000, 2002, 2013; Granath and Casero, 2004; Finetti et al., 2005). Small and large-scale paleogeographic recon- structions reveal that Sicily has been located along the African - European plate boundary from Paleozoic times (Ruiz-Martínez et al., 2012; Catalano et al., 2013; Berra and Angiolini, 2014; Scotese and Schettino, 2017). Starting from Triassic, the west-central Mediterranean platform (Apulia-Adria) was broken apart by the same tectonic pro- cesses that caused the opening of the Central Atlantic. After separation of north west Africa (northern Gondwana) from Eastern North America, Adria, Apulia (including Sicily) and southern Turkey continued to be part of the African Plate (Catalano et al., 2002, 2013; Robertson et al., 2003; Finetti et al., 2005; Berra and Angiolini, 2014; Scotese and Schettino, 2017). The extensional faulting was accompanied by regional and large-scale fissural basaltic volcanism at least since the Triassic. In- tercalations of mafic volcanics have been recorded in several wells of the Hyblean Plateau at different stratigraphic levels (Patacca et al., 1979; Rocchi et al., 1996; Granath and Casero, 2004; Finetti et al., 2005; Scotese and Schettino, 2017). Beginning in the Late Triassic, the whole Hyblean Plateau region was occupied by a wide shallow water carbonate platform (represented by the Sciacca Formation). The exten- sional phase related to the continental rifting caused the carbonate plat- form to break-up and this triggered the onset of a platform to basin system (Patacca et al., 1979; Brosse et al., 1988; Frixa et al., 2000). Shallow-water carbonate deposits (Noto Formation) covered the north- ern part of the area, while a deep anoxic-suboxic intraplatform basin de- veloped southward (Fig. 1). The Noto Formation (about 300 m thick) includes at least three interfingering facies. The first facies is spread throughout the Hyblean Plateau and consists of limestones (mudstones and wackestones), often dolomitized and recrystallized, interlayered with organic rich black shales. The second facies, is only found at the edge of the Plateau, is composed of wackestones, packstones and oolitic grainstones interpreted as beach ridge deposits (Patacca et al., 1979; Brosse et al., 1988). have been considered as beach ridge deposits (Patacca et al., 1979; Brosse et al., 1988). The third facies, named the Mila Member of the Noto Formation, occurs in the marginal area of the carbonate platform (Fig. 2). The Mila Member consists of two superimposed carbonate bodies, which backstep northwards, and are locally recrystallized and dolomitized. The lower microbial body lies above the carbonate platform of the Sciacca Formation, while the upper body overlies the lower microbial body (basinwards) and the Noto Formation (landwards, Frixa et al., 2000; Felici et al., 2014) (Fig. 2). As subsidence increased, sedimentation in the inner platform was mostly dominated by limestones and organic rich shales (still in- cluded in the Noto Formation; Frixa et al., 2000). At the same time, in the rapidly subsiding adjacent basin, a thick succession (Streppenosa Formation) deposited under suboxic-anoxic conditions. The thickness of the Streppenosa Formation is variable and reaches a maximum of about 3000 m in the southeastern part of the Hyblean Plateau. It has been subdivided into three members (Frixa et al., 2000). The Lower Streppenosa Member mainly consists of radiolarian-bearing muddy limestones with calciturbidites. Shale horizons occur in its lower portion. The Middle Streppenosa Member includes mudstones/wackestones, with intraclastic-peloidal and oolitic thin intercalations, often recrystal- lized or dolomitized, and black silty shales. The Upper Streppenosa Member consists of gray-green shales, marls and radiolarian-bearing muddy limestones with calcarenite intercalations. Compared with the Lower and Middle members, the silty shales and quartz siltstones in- crease, while the organic matter decreases (Frixa et al., 2000). Basalts and tuff layers occur in the sedimentary sequence at various strati- graphic levels and become more frequent in the Upper Streppenosa Member. On the basis of previous studies, basaltic horizons have an overall intraplate alkaline nature (Rocchi et al., 1996). The drowning of the carbonate platform-basin system first occurred with the spread of the basinal facies (Upper Streppenosa Member) over the marginal- inner platform complex, as also reported at a regional scale (Catalano et al., 2013). According to previous authors, the drowning phase first oc- curred in the Early Jurassic time (Patacca et al., 1979; Brosse et al., 1988; Frixa et al., 2000) (Fig. 3).

- Within this stratigraphic framework, the main elements of the Hyblean Plateau Petroleum System are as follows.
- Two reservoirs, represented by the carbonate platform succession (Sciacca Formation) and the marginal microbial mound complex (Mila Member). In the Sciacca Formation porosity reaches maxi- mum values of 20%, mostly due to fracturing (Mattavelli et al., 1969; Frixa et al., 2000). In the Mila Member, the poor reservoir properties are due to prevailing muddy facies but are improved by hydrothermal dolomitization, fracturing and karst.
- Two source rock units, represented by the Noto Formation whose Total Organic Carbon (TOC) reaches about 13% and by the Streppenosa Formation. Although the average TOC of the Streppenosa Formation is low (around 1%), its great thickness makes this formation a good source rock (Brosse et al., 1988; Frixa et al., 2000).
- One seal, consisting of the upper portion (Upper Streppenosa Mem- ber) of the Streppenosa Formation (Frixa et al., 2000).

The investigated wells, Streppenosa 1 and Bimmisca 1, were drilled in the northwestern and eastern parts of the Hyblean Plateau, respec- tively. The Streppenosa 1 well (36°50′45″N/02°16′09″E), reached a depth of 2908.4 m in the upper part of the Sciacca Formation. The Bimmisca 1 well (36°48′34″N/02°37′28″E) terminated at a depth of 3169 m within the Mila Member of the Noto Formation, and thus never reached the Sciacca carbonate platform. All the depths were mea- sured below the Rotary Table (MDBRT). The Streppenosa 1 and the Bimmisca 1 wells penetrated the inner area and the marginal complex of the carbonate platform-basin system, respectively (Figs. 1, 2). In this area, only the Upper Streppenosa Member is present, directly over- lying the Noto Formation (including the Mila Member). The complete Streppenosa Formation, including all the three members, is present only in the depocenter of the basin, and is penetrated by the Polpo 1 and Pachino 4 wells (Frixa et al., 2000; Cirilli et al., 2015) (Figs. 2, 3).

The succession investigated in the Streppenosa 1 borehole includes the Upper Streppenosa Member (2126 m–2452 m) and the Noto For- mation (2452 m–2825 m). In the Bimmisca 1 well, the succession investigated encompasses the Upper Streppenosa Member (2282 m– 2684 m) and the Noto Formation (2684 m–2803 m), including the Mila Member (2803 m–2879 m). The lowermost portion of the Mila Member, between 3169 m to 2908 m, has not yielded samples due to a loss of circulation. In both wells studied, the Streppenosa Formation is overlain by the pelagic deposits of the lower-middle Jurassic Modica Formation (Patacca et al., 1979), which is not included in this study.

3. Methods

Palynological and palynofacies analyses were carried out on a total of 59 cutting samples: 30 from the Streppenosa 1 well and 29 from the Bimmisca 1 well. The samples were processed using standard paly- nological techniques in order to obtain a final organic residue observ- able under a microscope (Green, 2001; Wood et al., 2002; Buratti and Cirilli, 2011). The palynomorphs and palynomacerals were visualized with a Leica DM1000 microscope using transmitted white light. Optical palynofacies analyses were conducted on the organic matter prior to ox- idation with nitric acid. The organic particles were classified according to the standard classification of Whitaker (1984), modified by Steffen and Gorin (1993). Marine and terrestrial palynomorphs were identified from both artificially oxidized and unoxidized residue.

For this study, only cuttings were available. A common problem with well cuttings is the potential contamination of rock fragments derived from uphole. This could represent a problem when interpreting both the palynostratigraphy and palynofacies. However, in our opinion, using a rigorous approach and method, conclusions can be drawn re- garding which palynological assemblages and palynofacies composition can be used as complementary tools. First, to identify the presence of caving contamination, we carefully handpicked the lithologies and com- pared them with up-hole samples. The identification was made on thin sections made up from cutting material, previously embedded in epoxy resin, observed under transmitted light microscope. Then we used the highest occurrences of taxa to define the tops of the palynozones. The first downhole occurrences (FDOs) of palynomorphs were used in con- structing the range charts, in order to minimize the error introduced by caving. The presence of a few anachronistic palynomorphs throughout the studied well succession indicated that contamination from caving was minimal. Thus we attempted to use the palynofacies composition and variation in order to reconstruct the depositional environment.

Palynomorphs and all the organic debris were measured quantita- tively. At least 250 particles per slide (two slides per sample) were counted and converted into percentages. Details on the sample process- ing, the general definition of the organic debris and the palynomorph quantitative analysis are given in the Online Resources. The palynologi- cal slides were then stored in the collection of the

Sedimentary Organic Matter Laboratory at the Department of Physics and Geology of the Perugia University (Italy).

4. Palynological data

A complete list of the identified taxa and data on quantitative analysis can be found in the Online Resource (Appendix I, Figs. S1; S2).

4.1 Palynology of the Streppenosa 1 well

The palynological assemblages in the Streppenosa 1 succession contain abundant sporomorphs in association with minor marine elements (microforaminiferal linings, dinoflagellate cysts and acritarchs) (Fig. 4, Pl.I). The microflora is dominated by *Classopollis meyerianus* and by trilete fern spores, such as *Deltoidospora mesozoica, Dictyophyllidites mortonii, Todiporites* sp., *Trachysporites fuscus,* which abundances vary throught the studied section, in association with minor *Acanthotriletes varius*, *Baculatisporites* sp., *Calamospora tener*, *Carnisporites spiniger*, *Densosporites fissus, Kraeuselisporites* sp. and *Porcellispora longdonensis.* The distribution of *Limbosporites lundbladiae*, *Perinopollenites elatoides*, and bisaccate pollen grain as *Klausipollenites gouldii* is not constant throughout the well. The microflora gradually diversify throughout the Upper Streppenosa Member with the first downhole occurrences (FDOs) of *Punctatisporites fungosus, Paraklukisporites foraminis, Classopollis torosus* and *Striatella seebergensis* in its upper part, and of *Trachysporites fuscus*, *Cingulizonates rhaeticus, Densosporites foveocingulatus*, and *Ricciisporites* sp., in its central-lower part. The FDO of the index species *Ischyosporites variegatus* is recorded in the central-upper part (2235.5 m) whereas that of *Porcellispora longdonensis* in the lower portion (2421.5 m) of the member. The presence of *Leptolepidites major, Pilosisporites* sp. and *Trilobosporites aequiverrucosus* is considered here as caving. *Ischyosporites variegatus* in association with *Polypodiisporites polymicroforatus*, *Retitriletes semimuris, Triancoraesporites ancorae*, rare *Araucariacites australis* have their last downhole occurrences (LDO) at the base of the Upper Streppenosa Member (sample at

2445.5 m) and are not recorded in the underlying Noto Formation. The assemblage from the Noto Formation is less diversified and records few FDOs in the central-upper part: the FDO of *Eucommiidites* sp. at 2503.5 m and that of *Tsugaepollenites psudomassulae* at 2555.5 m. The fresh water chlorococcale alga *Botryococcus* sp. is more or less constantly present from the middle part of the Noto Formation slightly decreasing upward, while *Schizosporis scissus* is recorded only at the base of the member. Microforaminiferal linings are constantly present within the investigated well section. Acritarchs and dinoflagellate cysts are rare and commonly poorly preserved. The FDO of *Suessia swabiana* is recorded at the base of the Upper Streppenosa Member.

4.2 Palynology of the Bimmisca 1 well

As in the Streppenosa 1 well, the palynological assemblages from Bimmisca 1 well are dominated by sporomorphs in association with minor marine components (Fig. 5, Pl.II). The FDO of *Ischyosporites variegatus* is recorded at the top of the studied well section (2302 m) with *Araucariacites australis* and *Deltoidospora mesozoica* and, 19 m below, by *Calamospora tener*. The assemblage diversity and abundance progressively increase downhole with the FDO of *Classopollis meyerianus* at 2481 m. The middle portion of the Upper Streppenosa Member is characterized by the FDO of some important taxa such as *Polypodiisporites polymicroforatus, Convolutispora klukiforma*, cf. *Retitriletes semimuris*, *Annulispora folliculosa, Limbosporites lundbladiae,* cf. *Retitriletes austroclavatidites, Trachysporites fuscus, Acanthotriletes varius, Camarozonosporites rudis, Densosporites foveocingulatus, Leptolepidites reissingeri*. The FDO of the species index *Porcellispora longdonensis* is recorded at 2603 m and that of *Classopollis torosus* at 2610 m.

Overall, the fern spores are abundant in the Upper Streppenosa Member and and can be found throughout the well section. The alga *Botryococcus* sp. is occasionally present in the middle part of the Upper Streppenosa Member. Microforaminiferal linings, although low abundant, become more constant in the Upper Streppenosa Member. The FDO of *Suessia swabiana* is recorded at the base of the Upper Streppenosa Member, where it is low abundant. The assemblage diversity decreases in the Noto Formation. A few FDOs are recorded in its lower portion as for the spores *Conbaculatisporites* sp., *Conbaculatisporites spinosus* and *Punctatisporites fungosus*.

5. Palynofacies and lithofacies data

The use of palynofacies, combined with other approaches, can pro- vide useful information on sedimentary processes and on the chemical and ecological parameters of the depositional environment, such as, ox- ygenation, length of transportation, water energy and nutrient level (van der Zwan, 1990; Steffen and Gorin, 1993; Hart et al., 1995; Tyson, 1995, 2001; Batten and Stead, 2007). The abundance of total terrestrial organic matter commonly decreases with the distance from the land- masses and the parent flora. More labile components (i.e. cutinite) are rapidly degraded during transport, while oxidized particles (i.e. inertinite) can be widely distributed into marine basins because they are refractory to further biochemical oxidation. In a marine setting, the narrow width of the continental shelf, as expected for the study area, exerts a strong control on the relative positions of proximal and distal environments (Mascle et al., 1996). Important controlling factors on organic matter accumulation and preservation rate include the pri- mary productivity and the oxygen level of the water column. Under suboxic-anoxic conditions, the organic matter is usually converted into amorphous organic matter (AOM). Given that AOM is highly sus- ceptible to oxidation, its presence can be a proxy for the low oxygen content of the water column and sediment water interface (Tyson, 1995; Batten and Stead, 2007). The relative abundances of sedimentary organic matter and palynofacies composition from the Streppenosa 1 and the Bimmisca 1 wells are plotted in Figs. 6 and 7. Additional infor- mation on the general characteristic of organic debris is provided in the Online Resources.

5.1 Streppenosa 1 well

Six intervals, characterized by different lithofacies and palynofacies, were distinguished in this well. Lithology and stratigraphic distribution of the palynofacies ratios as well as the number and spacing of analyzed samples for each interval are illustrated in Fig. 6.

- Interval I (Palynofacies A, Pl. III.1) (2824 m – 2735.5 m) represents the lowest part of the Noto Formation. The interval mainly consists of shales and thin bedded limestones. The palynofacies contains abundant inertinite, which reaches the highest values in the upper part of the interval (58%). Vitrinite 1 abundance decreases from bottom to top (32% to 8%). The amount of vitrinite 2 is almost constant within the interval (7% to 10% upwards). Cutinite, sporomorphs (tetrads included) have a low frequency (less than 5%). Marine components are rare and mainly represented by microforaminiferal linings in the lower part. A few specimens of the freshwater alga *Botryococcus* sp. were recorded in the upper part of the interval. The AOM abundance increases from the base (4%) to the central part (20%) and decreases (15%) at the upper part of the interval .

- Interval II (Palynofacies B, Pl. III.2) (2735.5 m – 2624.5 m) consists of limestones intercalated with shales, which become more frequent in the upper part. Vitrinite 1 abundance increases from the lower (38%) to the central part of the interval (58%), and decreases upwards (15%), except for at the interval 2637.5. Inertinite and vitrinite 1 abundances show general opposite trends being inertinite lower where vitrinite 1 higher and vice versa. The vitrinite 2 content is overall low, ranging from 2.5% to 12.5%. Sporomorphs, tetrads included, relatively increase in the central part of the interval (up to 15%), cutinite amount is low (less than 2%) within the interval. Microforaminiferal linings and *Botryococcus* sp. slightly increase upwards (up to 5%). The highest AOM values (up to 30%) are recorded in the shaly beds at the lower part of the interval.

- Interval III (Palynofacies C, Pl. III.3) (2555.5 m – 2476.5 m), overlying a basalt horizon, is composed of thich shaly horizons alternated to limestone. Inertinite and vitrinite 1 fluctuate along the interval with a peak of respectively 54% and 45%, showing an opposite trend. Vitrinite 2 abundance ranges between 8% to 16%. The amount of cutinite slightly increases in respect to the underlying interval (up 6%), that of sporomorphs slightly decreases and tetrads are few. The AOM reaches the maximum value (30%) within the shaly intervals in correspondence of the lowest value of vitrinite 1 and moderate amount of inertinite. Microforaminiferal linings are few. A few specimens of *Botryococcus* sp. are recorded only in the lower and central part of the interval.

- Interval IV (Palynofacies D, Pl. III.4) (2476.5 m – 2409.5 m) includes the Noto Formation and Upper Streppenosa Member boundary (at 2452.5 m depth). The interval exhibits a basal thick carbonate horizon (Noto Formation) passing upwards into alternations of dark grey shales and limestones containing fine grained calcarenites (Upper Streppenosa Member). The palynofacies shows the highest values of AOM (up to 40%) at the lower and at the upper part of the interval, the latter is combined with high values of pyrite framboids. In the central part of the interval, AOM abundance decreases up to 5%. There is a progressive upward increase in vitrinite 2 (10% to 35%) accompanied by a decrease in vitrinite 1 (28% to 6%), while inertinite values remain almost constant. The sporomorph abundance, tetrads included, shows a peak in the central part of the interval (up to 25%). Cutinite amount fluctuates from low values (1.5%) in the central part and relative higher values at the lower and upper part of the interval. Constant low percentage (5%) of marine elements (microforaminiferal linings and few dinoflagellate cysts) has been recorded in the central and upper part of the interval. Low amount of *Botryococcus* sp. is present at the base and at the top of the interval.

- Interval V (Palynofacies E, Pl. III.5) (2409.5 m – 2308.5 m) consists of black shales in the lower part passing, upwards, to thick carbonate beds, which contain calcarenites, interbedded with shaly intervals and radiolarian bearing muddy limestones. The low number of samples prevented a detailed palynofacies characterization of this interval that has been possible only from 2357.5 m to 2308.5 m. Inertinite reaches the highest values (55%) at the base of the sampled interval, where all the other palynomacerals and sporomorphs decrease. Vitrinite 1 slightly increases upwards (up to 25%), while vitrinite 2 abundance remains constant (15%) as well as cutinite and sporomorphs although occurring in low abundance. The AOM values increase in the upper part of the interval (25%) within the shaly interval. A few microforaminiferal linings (1.8%) are present.

- Interval VI (Palynofacies F, Pl. III.6; IV.1) (2308.5 m – 2147.5 m) is dominantly carbonate except for a basal thick dark shaly horizon and thin intercalations of dark shales within carbonates. The carbonate horizons consist of thin bedded limestone mostly characterized by radiolarian and thin shelled bivalve bearing mudstone-wackestone. Due to the lack of samples, the palynofacies analysis has been possible starting from the central part of this interval. Vitrinite 1 and sporomorphs record the highest value in the central part of the interval (58% and 22% respectively). Vitrinite 2 abundance fluctuates within the interval (8% to 20%) as well as cutinite (5% to 10%). The AOM shows the highest value in the central part of the interval (40%), whereas pyrite is present only in the central (16%) and upper (6%) part. The percentage of microforaminiferal linings increases upwards and *Botryococcus* sp. is consistently present (10%) at the topmost interval.

5.2 Bimmisca 1 well

Five intervals and related lithofacies and palynofacies were recognized. Lithology and stratigraphic distribution of the palynofacies ratios, the number and spacing of analyzed samples are illustrated in Fig. 7.

- Interval I (Palynofacies G, Pl. IV.2) (2879 m – 2823 m), in the Mila Member, composed mainly of microbial dolostones. Terrestrial organic debris dominates the palynofacies. Vitrinite 1 reaches high values (73%) in the central-upper part of the interval, whereas vitrinite 2 ranks at low percentages (around 5%). Few sporomorphs are present (1.5%). Cutinite abundance shows moderate value (19%) at the base of the interval and decreases upwards. Inertinite and AOM values show the same pattern progressively decreasing upwards (40% to 5%, inertinite; 38% to 15%, AOM). Microforaminiferal linings and acritarchs are few (1%).

- Interval II (Palynofacies H, Pl. IV.3) (2823 m – 2694 m) mostly belongs to the Noto Formation overlying the Mila Member. It consists of dolostones intercalated with minor shales. Vitrinite 1 and inertinite fluctuate (10% up to 80%) within the interval showing an opposite trend. Vitrinite 2 abundance is almost constant ranging from 3% to 7%. Similarly the amount of cutinite remains more or less constant within the interval. Sporomorph abundances (tetrad included) show variations along the interval never exceeding the 18%. The AOM values are variable (25% to 2%) showing an overall decreasing trend upward. Microforaminiferal linings and acritarchs are few (up to 2%).
- Interval III (Palynofacies I, Pl. IV.4) (2694 m – 2603 m). The base of this interval coincides with the Noto Formation - Upper Streppenosa Member boundary. The interval is marked by an abrupt decrease in carbonate content, being dominated by shales with thin muddy carbonate intercalations. Overall, the palynofacies shows an increase in the total amount of continental organic debris and a decrease in AOM (from 20% to 2% upwards). Inertinite and vitrinite 1 show strong fluctuations, the former reaching the highest values in the carbonate beds. Vitrinite 2 ranks at low abundance (2% to 10%) as well as cutinite. Sporomorphs and tetrads increase upwards ranking at 32%, the highest value recorded within the well section. Marine palynomorphs (microforaminiferal linings, acritarchs and few dinoflagellate cysts) slightly increase in respect to the underlying intervals.
- Interval IV (Palynofacies L, Pl. IV.5) (2603 m – 2441 m) consists of shales with minor intercalations of carbonate composed of thin bedded muddy limestone. The palynofacies is dominated by inertinite (up to 92% in the upper part of the interval). The other palynomacerals and sporomorphs are low to absent, except for moderate value of vitrinite 1 (up to 30%). AOM content is low (less than 8%) and further decreases to disappear upwards. Pyrite (8%), marine components (not more than 5%) such as

microforaminiferal linings and rare acritarchs are present in the lower part. *Botryococcus* sp. has been recorded only in this interval.

- Interval V (Palynofacies M, Pl. IV.6) (2342 m – 2302 m.) overlies a basalt horizon. It consists of shale and thin bedded muddy limestone alternations. Palynofacies is dominated by inertinite (45% to 84%) and vitrinite 1 (up to 45%), combined with low amount of other palynomacerals and sporomorphs. Tetrads are absent. The abundance of AOM is low (up to 6%) as well as that of pyrite (up to 2%), this latter found only in the upper part of the interval. A few microforaminiferal linings and acritarchs are present (up to 4%).

6. Discussion

6.1 Palynostratigraphic assessment and dating

The Noto Formation and the Upper Streppenosa Member can be assigned to the Rhaetian age given the abundance of *Classopollis* species (*Classopollis meyerianus* and minor *Classopollis torosus*) in assemblage with other index species such as *Ischyosporites variegatus, Porcellispora longdonensis* and *Trachysporites fuscus*. These species have been found in typical Rhaetian strata from several localities (Morbey, 1975; Schuurman, 1977; Barrón et al., 2006; Kürschner et al., 2007; Warrington et al., 2008; Ruhl et al., 2009; Cirilli, 2010; de Jersey and McKellar, 2013; Hillebrant et al., 2013; Lindström, 2016; Lindström et al., 2017b). Palynological assemblages with similar compositions have been recorded from Southern Alps and Apennines in Italy (Cirilli et al., 1994; Galli et al., 2007) and in some southern Mediterranean areas such as Tunisia, Libya, Algeria, Morocco (Adloff et al., 1986; Yaroshenko, 2007; Cirilli, 2010). Palynological assemblages from Northern Spain (Asturias) and France, although showing some common elements (e.g. dominance of *Classopollis* spp. and fern spores) differ for the presence of *Ricciisporites tuberculatus* (Barrón et al., 2006; Gómez et al, 2007). The absence of *R. tuberculatus* could be related to the palaeogeographic position of Sicily during Late Triassic along the

African- European plate boundary, under warm paleoclimatic conditions (Ruiz-Martínez et al., 2012; Catalano et al., 2013; Berra and Angiolini, 2014; Scotese and Schettino, 2017). Recent data have documented that the gymnosperm pollen *R. tuberculatus* appears to be more restricted to the Northern Hemisphere (Kürschner et al., 2014; Lindström, 2016; Lindström et al., 2017a). Its abundance seems to be vicariant with that of *Classopollis*, being less common or absent where *Classopollis* is abundant, as in the present case, revealing different ecological and/or climatic preferences. In the GSSP stratotype Kuhjoch section (Karwendel Mountains, Austria) the lowest occurrences of *I. variegatus* and *Cerebropollenites thiergartii,* which is considered the best marker for the T-J boundary, are recorded several meters below the first appearance of the ammonite *Psiloceras spelae* defining the base of the Hettangian (Bonis et. al. 2009; Kürschner and Herngreen, 2010; Hillebrant et al., 2013). Therefore, the presence of *I. variegatus* without *C. thiergartii* and in association with *Classopollis* spp*., P. longdonensis* and *Kraeuselisporites reissingeri,* led tentatively to refer part of the Upper Streppenosa Member to the lowermost part of the *Trachysporites–Heliosporites* Zone (TH) which is considered as Rhaetian (Hillebrant et al., 2013). The thickness of the interval below the FO of the *C. thiergartii* depends from the sedimentation rate which surely was not the same for all the sections bracketing the T/J boundary. In this case study, considering the high subsidence rate caused by synsedimentary tectonic activity and the medium-to high sedimentation rate (Patacca et al., 1979), the presence of *C. thiergartii* in the upper part of the Upper Streppenosa Member cannot be excluded. However its presence has not been recorded either in these two wells or in the Pachino 4 well (Cirilli et al., 2015). The microfloral content recorded in the lower part of the Upper Streppenosa Member and in the Noto Formation dominated by *Classopollis meyerianus* in association with *T. fuscus*, *P. longdonensis, Kraeuselisporites* sp. and *Polypodiisporites polymicroforatus* could be correlated with the *Trachysporites–Porcellispora* Zone (TPo) considered as latest Rhaetian as defined in the Tiefengraben section and Northern Calcareous Alps, Austria, (Kürschner et al. 2007; Hildebrandt, 2013). The age attribution of the whole studied well section to latest Rhaetian would explain also the lack of *Patinasporites densus* and *Enzonalasporites vigens* which seems to have their last occurrences in the uppermost Norian-lower Rhaetian (Cirilli, 2010 for references). In Sicily these two species have been recorded in independently dated Carnian and Norian strata both from outcrops and subsurface (Visscher and Krystyn, 1978; Buratti and Carrillat, 2002; Trincianti et al., 2015).

By correlating the new palynological data with those of Pachino 4 well (Cirilli et al., 2015), it results that the deposition of Noto Formation, at the marginal and inner carbonate platform-basin system, may be considered coheval with the Middle Streppenosa Member deposited in the deepest part of the basin. Furthermore, it implies that the initial drowning phase of the carbonate-basin system (Upper Streppenosa Member) can be predated to Rhaetian. The previous age attribution as Early Jurassic of the whole Upper Streppenosa Member (Fig. 3) was based on the presence of the calcareous nannofossil *Schizosphaerella punctulata* and on a palynological assemblage dominated by *Classopollis classoides* and *C. meyerianus* and (Frixa et al., 2000). However, although *S. punctulata* was most common in the Early Jurassic times its range spans from the latest Triassic to the end of the Jurassic (Perch-Nielsen, 1989). In St Audrie's Bay (England), *S. punctulata* first occurs about one metre below the candidate Hettangian GSSP level (in Blue Lias Formation bed 7). Its occurrence slightly predates the base of the *Psiloceras planorbis* Zone and correlates with the onset of the main negative excursion in $\delta^{13}C_{org}$ values (Hesselbo et al., 2002, 2004). Additionally, the relative abundance of *Classopollis* spp., which is also present in the Triassic, does not justify assigning a Jurassic age to the Upper Streppenosa Member, given that in this case *Classopollis* spp. do not occur alongside typical Jurassic forms.

6. 2 Palaeoenvironment, palaeoclimate and depositional model

Considering the general paleogeographic and paleoenvironmental settings, the lateral and vertical variations of palynofacies and lithofacies and the prevailing continental organic matter across the well sections indicate a deposition in a marine environment, proximal to the terres- trial source area, under variable energy and redox conditions.

The Noto Formation, crossed by the Streppenosa 1 well, located in the inner part of the carbonate platform-basin system, has a clear cyclic arrangement. Each interval shows a trend characterized by a decreasing AOM and palynomaceral and sporomorph increasing upwards. The rel- ative abundance of AOM in the basal part of each interval results from a combination of good preservation, related to suboxic–anoxic condi- tions, and low-energy environments. It has also resulted in the deposi- tion of laminated shales with few limestone intercalations. The upper part of each interval shows shallower, and relatively better oxygenated, conditions where particulate organic matter dominates over AOM, which was presumably destroyed by oxidation and biodegradation. In the Bimmisca 1 well, which penetrates the platform marginal area, the palynofacies fluctuations are more evident at the scale of the entire suc- cession (Noto Formation/Mila Member and Upper Streppenosa Mem- ber), in accordance with lithofacies variation from mainly carbonate to predominantly shaly upwards. The increase in inertinite and the de- crease in terrestrial particulate organic matter and AOM from bottom to top are consistent with a shift from the proximal to distal position of the platform-basin system with respect to the landmasses. The moderate-to-high value of AOM recorded in the shallow water micro- bial mounds of the Mila Member could be partially related to the micro- bial community itself. Under microbial proliferation, the extracellular polymeric substances (EPS) form a well–defined protective envelope around cyanobacteria cells, which protect AOM from the oxidation pro- cesses (Sutherland, 2001; Pacton et al., 2007). The overall deepening trend of the platform-basin system culminated with the deposition of the Upper Streppenosa Member. In each interval, palynofacies signa- tures clearly reflect the lithofacies variations, which consist of thick shaly beds and minor limestones containing calcarenite intercalations: dominant AOM and minor inertinite in the shaly intervals, highest amount of inertinite and lowest amount of AOM within limestones. These fluctuations could be interpreted as a result of changes in water energy and oxygen content. The higher energy and good oxygenated conditions during the calciturbidites deposition destroyed the AOM and reduced the preservation rate of particulate OM, except inertinite, which is the most resistant palynomaceral. The scarce benthic fauna living at such deep marine bottoms may also have played a role. On the other hand, the suboxic-anoxic conditions, during the deposition of finely laminated shales, promoted the AOM preservation. The concur- rent AOM decrease and inertinite increase upwards confirm the gradual and relative deepening of the depositional environment, highlighted by the basinal facies of the Upper Streppenosa Member onlapping and overlying the microbial mound (Mila Member) at the margin complex and the inner suboxic lagoonal facies of the Noto Formation. The increased deepening and the facies onlapping have been widely reported at the regional scale (Catalano et al., 2013). The drowning phases of the carbonate platform-basin system were accompanied by depositional environment shifting from proximal to distal conditions with respect to the landmasses and parent flora. This is highlighted in both wells by the palynofacies signatures, and the decrease, upwards, of the total terrestrial organic debris (i.e. vitrinite, cutinite and sporomorphs, tet- rads included) with the exception of inertinite. Given that inertinite is the most resistant palynomaceral, it can be transported for a long dis- tance from the continent and settled from suspension in a low-energy, offshore environment (Steffen and Gorin, 1993). Based on the data ob- tained and correlated with data from the Pachino 4 well, belonging to the same petroleum system and discussed in a previous paper (Cirilli et al., 2015), the paleoenvironmental evolution of the entire platform- basin system could be interpreted in terms of an “expanding puddle model” (sensu Wignall, 1991; Wignall and Newton, 2001). This model suggests the development of anaerobic conditions within relative shal- low intra-cratonic confined basins, with deposition of organic rich sed- iments both in the deepest part of the basin (i.e. Pachino 4 well, Cirilli et al., 2015) and in the shallow marine areas close to the margin of the carbonate platform (crossed by the Streppenosa 1 and the Bimmisca 1 wells) colonized by microbial mounds (Mila Member) (Fig. 2). During the Rhaetian, as marine transgression continued, the inner peritidal area of the carbonate platform started to drown under permanent subtidal water conditions, with episodes of low oxygenation (Noto For- mation). However, the carbonate factory continued to produce, as dem- onstrated by the calcarenite intercalations within the organic rich facies deposited in the adjacent basin. The platform margin setting facilitated the development of toe-of-slope aprons characterized by calciturbidites, intercalated with organic rich shales. At the same time, as observed in the Pachino 4 well (Cirilli et al., 2015), in the deepest part of the basin, thick organic rich shales and limestones sedimented. Subsequently, the maximum rise in sea level, combined with the increase in subsi- dence caused the expansion of deep waters and the spread of organic rich facies over the marginal-inner platform complex. This step corre- sponds to the deposition of the Upper Streppenosa Member in the basin depocenter (cf. Pachino well in Cirilli et al., 2015) until onlapping the marginal and inner part of the preexisting carbonate platform. According to our palynological data, the initial drowning of the carbonate-platform can be dated as Rhaetian. Intense tectonic activity related to the continental rifting (and on a larger scale to the Pangea fragmentation) on the northern edge of the African craton (Ruiz- Martínez et al., 2012; Catalano et al., 2013; Berra and Angiolini, 2014; Scotese and Schettino, 2017) was the main cause of the sea level varia- tions in the western Tethys area. In the meantime increasing humidity led to increased freshwater input in the sedimentary basin. This is suggested by the combined presence of fern spores and chlorococcale algae (*Botryococcus*) whose occurrence in marine deposits tends to indicate freshwater incursions (Batten and Grenfell, 1996). This is also demon- strated by the abrupt increase in clay content, found in the middle-upper portion of the well sections. The main cause for this abrupt cli- mate change could be due to the degassing of basalt flows from the CAMP (van de Schootbrugge et al., 2009; Bonis et al., 2010; Schoene et al., 2010; Ruhl et al., 2011; Schaller et al., 2011; Lindström et al., 2012, 2017b; Pálfy and Zajzon, 2012; Bond and Wignall, 2014;Fijałkowska-Mader, 2015; Davies et al., 2017). The increasing atmospheric CO2 concentrations created up to 3–4° in warming, thus leading to a substantial increase in atmospheric water vapor. Consequently the huge amount of greenhouse-gas emissions in the atmosphere and in the ocean waters could be the main cause of the mass extinction at the end of Triassic. Recent data (Davies et al., 2017; Lindström et al., 2017b) date the onset of the CAMP magmatic activity to about 1000kyr before the earliest known eruptions, showing clear evidence of a strict relation be- tween CAMP, increasing humidity and ETE. The location of Sicily in the northern area of the African Plate during the Late Triassic, suggests that the effects of CAMP degassing could have also affected this area.

7. Conclusions

The results of the integrated palynostratigraphy, palynofacies and lithofacies data from the studied well sections shed new light on the Early Mesozoic evolution of the Hyblean Plateau and on the factors trig- gering the organic matter accumulation and preservation in these kinds of intraplatform basins. The palynological assemblages enable the age of the source and seal rocks to be defined and to characterize the timing of the drowning phases of the carbonate platform-basin system. Based on the new palynological data, the entire succession (Noto Formation and Upper Streppenosa Member), can be dated as Rhaetian, thus constraining the initial drowning phase of the carbonate-basin system along a time in- terval characterized by increasing global humidity, related to the degassing of basalt flows from the CAMP. Climate-driven fluctuations in continental runoff controlled anoxia and black shale deposition in the Triassic Hyblean basin. Humid phases characterized by high precipitation, strong chemical weathering, and freshwater runoff from landmasses caused water stratification and subsequent anoxia at marine bottoms, fa- cilitating the preservation of sedimentary organic matter. The humid phase is highlighted by the increase in clay content and by the presence of fern spores and *Botryococcus* algae. The integrated palynofacies and lithofacies data highlighted a paleogeographic scenario, consisting of a platform-basin system whose evolution was strongly controlled by rela- tive sea level changes triggered by a combination of tectonic and climate factors. Both palynofacies and lithofacies patterns clearly reflect a meter- scale cyclicity in the succession. The paleoenvironmental history of the Hyblean area was strongly marked by a progressive sea-level rise during the Upper Triassic. This is highlighted by the vertical arrangement of cy- cles showing a deepening-upward trend, which culminated with the drowning of the carbonate platform and the spread of organic rich facies over the marginal-inner platform, at the end of the Triassic. This study demonstrates how palynofacies analysis can be used as important com- plementary tool in determining the depositional environment and to de- cipher paleoenvironmental and paleoclimatic changes.

Supplementary data to this article can be found online at https://doi.org/10.1016/j.revpalbo.2018.04.003.

Acknowledgments

The authors gratefully acknowledge Eni Upstream and Technical Services Management for permission to study the cutting samples of the Bimmisca1 and Streppenosa 1 boreholes and to publish the results. Thanks to Amalia Spina and Enrico Capezzuoli for their useful discussions and suggestions. The authors are deeply greatful for helpful comments from Sofie Lindström, from an anonymous reviewer and from the editor Mike Stephenson. Their comments and suggestions surely improved the quality of this article. This study was supported by the funds of the Sedimentary Organic Matter Laboratory (Grant number: CONLABSSOR-000934), directed by S. Cirilli (Perugia University, Italy).

References

Adloff, M.C., Doubinger, J., Massa, D., Vachard, D., 1986. Trias de Tripolitaine (Libye). Nouvelles données bios- tratigraphiques et palynologiques. Revue de l'Institut Francais du Petrole 41, 27-72.

Barrón, E., Gómez, J.J., Goy, A., Pieren, A.P., 2006. The Triassic–Jurassic boundary in Asturias (northern Spain): palynological characterization and facies. Review of Palaeobotany and Palynology 138, 187–208.

Batten, D.J. and Grenfell, H.R., 1996. *Botryococcus*. In: Jansonius, J., McGregor, D.C. (Eds.), Palynology: Principles and Applications. American Association of Stratigraphic Palynologists Foundation, v. 1, pp. 205-214.

Batten, D.J., Stead, D.T., 2007. Palynofacies Analysis and Its Stratigraphic Application. In: Koutsoukos, E.A.M. (Ed.), Applied Stratigraphy. Springer Dordrecht, Netherlands, pp. 203–226.

Berra, F., 2012. Sea-level fall, carbonate production, rainy days: How do they relate? Insight from Triassic carbonate platforms (Western Tethys, Southern Alps, Italy). Geology 40, 271–274.

Berra, F., Angiolini, L., 2014. The evolution of the Tethys region throughout the Phanerozoic: A brief tectonic reconstruction. In: Marlow, L., Kendall, C., Yose, L. (Eds.), Petroleum systems of the Tethyan region: AAPG Memoir 106, pp. 1- 27.

Bond D.P.G., Wignall P.B., 2014. Large igneous provinces and mass extinctions: an update. In: Keller, G., Kerr, A.C., (Eds.), Volcanism, Impacts, and Mass Extinctions: Causes and Effects: Geological Society of America Special Paper 505, pp. 29-55.

Bonis, N.R., Kürschner, W.M., 2012. Vegetation history, diversity patterns, and climate change across the Triassic/Jurassic boundary. Paleobiology 38, 240–264.

Bonis, N.R., Kürschner, W.M., Krystyn, L., 2009. A detailed palynological study of the Triassic–Jurassic transition in key sections of the Eiberg Basin (Northern Calcareous Alps, Austria). Review of Palaeobotany and Palynology 156, 376–400.

Bonis, N.R., Ruhl, M., Kürschner, W.M., 2010. Climate change driven black shale deposition during the end-Triassic in the western Tethys. Palaeogeography, Palaeoclimatology, Palaeoecology 290, 151–159.

Brosse, E., Loreau, J.P., Huc, A.Y., Frixa, A., Martellini, L., Riva, A., 1988. The organic matter of interlayered carbonates and clays sediments - Trias/Lias, Sicily. Organic Geochemistry 13, 433–443.

Buratti, N., Carrillat, A., 2002. Palynostratigraphy of the Mufara Formation (Middle–Upper Triassic, Sicily). Rivista Italiana di Paleontologia e Stratigrafia 108, 101–117.

Buratti, N., Cirilli, S., 2011. A new bleaching method for strongly oxidized palynomorphs. Micropaleontology 57, 263-267.

Catalano, R., Doglioni, C., Merlini, S., 2000. On the Mesozoic Ionian Basin. Geophysical Journal International 143, 1-24.

Catalano, R., Merlini, S., Sulli, A., 2002. The structure of western Sicily, central Mediterranean. Petroleum Geoscience 8, pp-7-18.

Catalano, R., Valenti, V., Albanese, C., Accaino, F., Sulli, A., Tinivella, U., Morticelli, M.G., Zanolla, C., Giustiniani, M., 2013. Sicily's fold-thrust belt and slab roll-back: The SI.RI.PRO. Seismic crustal transect. Journal of the Geological Society 170, 451-464.

Cirilli, S., 2010. Upper Triassic–Lowermost Jurassic Palynology and Palynostratigraphy: A Review. In: Lucas, S.G. (Ed.), The Triassic Timescale 334. Geological Society, Special Publications, London, pp. 285–314.

Cirilli, S., Bucefalo-Palliani, R., Pontini, M. R., 1994. Palynostratigraphy and palynofacies of the Late Triassic *R. contorta* facies in the Northern Apennines: II. The Monte Cetona Formation. Revue de Paléobiologie 13, 319–339.

Cirilli, S., Marzoli, A., Tanner, L., Bertrand, H., Buratti, N., Jourdan, F., Bellieni, G., Kontak, D., Renne, P.R., 2009. Latest Triassic onset of the Central Atlantic Magmatic Province (CAMP) volcanism in the Fundy Basin (Nova Scotia): new stratigraphic constraints. Earth and Planetary Science Letters 286, 514–525.

Cirilli, S., Buratti, N., Gugliotti, L., Frixa, A., 2015. Palynostratigraphy and palynofacies of the Upper Triassic Streppenosa Formation (SE Sicily, Italy) and inference on the main controlling factors in the organic rich shale deposition. Review of Palaeobotany and Palynology 218, 67-79.

Clémence, M.E., Bartolini, A., Gardin, S., Paris, G., Beaumont, V., Page K. N. 2010. Early Hettangian benthic–planktonic coupling at Doniford (SW England): Palaeoenvironmental implications for the aftermath of the end-Triassic crisis. Palaeogeography, Palaeoclimatology, Palaeoecology 295, 102–115.

Dal Corso, J., Marzoli, A., Tateo, F., Jenkyns, H.C., Bertrand, H., Youbi, N., Mahmoudi, A., Font, E., Buratti, N., Cirilli, S, 2014. The dawn of CAMP volcanism and its bearing on the end-Triassic carbon cycle disruption. Journal of the Geological Society of London 171, 153-164.

Davies, J.H.F.L., Marzoli, A., Bertrand, H., Youbi, N., Ernesto, M., Schaltegger, U., 2017. End-Triassic mass extinction started by intrusive CAMP activity. Nature Communications 8, 1-8.

de Jersey, N.J., McKellar, J.L., 2013. The palynology of the Triassic–Jurassic transition in southeastern Queensland, Australia, and correlation with New Zealand. Palynology 37, 77–114.

Felici, E., Frixa, A., Maragliulo, C., Cirilli, S., 2014. The Mila Mb. of Noto Fm.: an integrated method to characterize a Triassic microbial reservoir rock (SE Sicily, Italy). Rendiconti On Line della Società Geologica Italiana Suppl. 1, Vol. 31.SGI - SIMP Congress (Abstract Book).

Fijałkowska-Mader, A., 2015. A record of climatic changes in the Triassic palynological spectra from Poland. Geological Quarterly 59, 615-653.

Finetti I.R., Lentini F., Carbone S., Del Ben A., Di Stefano A., Forlin E., Guarnieri P., Pipan M., Prizzon A., 2005. Geological Outline of Sicily and Lithospheric Tectono-Dynamics of its Tyrrhenian Margin from New CROP Seismic Data. In: Finetti, I.R. (Ed.), “CROP Deep Seismic exploration of the Central Mediterranean and Italy”. Elsevier, Special Volume, pp. 319-376.

Frixa, A., Bertamoni, M., Catrullo, D., Trinicianti, E., Miuccio, G., 2000. Late Norian – Hettangian palaeogeography in the area between wells Noto 1 and Polpo 1 (S-E Sicily). Memorie della Società Geologica Italiana 55, 279 – 284.

Galli, M. T., Jadoul, F., Bernasconi, S. M., Cirilli, S., Weissert, H., 2007. Stratigraphy and palaeoenvironmental analysis of the Triassic–Jurassic transition in the western Southern Alps (Northern Italy). Palaeogeography, Palaeoclimatology, Palaeoecology 244, 52–70.

Gómez, J. J., Goy, A., Barrón, E., 2007. Events around the Triassic–Jurassic boundary in northern and eastern Spain: a review. Palaeogeography, Palaeoclimatology,Palaeoecology 244, 89–110.

Granath, J. W., Casero, P., 2004. Tectonic setting of the petroleum systems of Sicily. In: Swennen, R., Roure, F., Granath, J.W. (Eds.), Deformation, fluid flow, and reservoir appraisal in foreland fold and thrust belts. AAPG Hedberg Series 1, pp.391–411.

Green, O.R., 2001. A manual of practical laboratory and field techniques in palaeobiology. Dordrecht. Kuwer Academic Publishers.

Haas, J., Götz, A.E., Pálfy, J., 2010. Late Triassic to Early Jurassic palaeogeography and eustatic history in the NW Tethyan realm: New insights from sedimentary and organic facies of the Csővár Basin (Hungary). Palaeogeography, Palaeoclimatology, Palaeoecology 291, 456–468.

Haas, J., Budai, T., Raucsik, B., 2012. Climatic controls on sedimentary environments in the Triassic of the Transdanubian Range (Western Hungary). Palaeogeography, Palaeoclimatology, Palaeoecology 353-355, 31-44.

Harris, N.B., 2005. The Deposition of Organic-Carbon-Rich Sediments: Models, Mechanisms, and Consequences — Introduction. In: Harris, N.B. (Ed.), The Deposition of Organic carbon-rich Sediments: Models, Mechanisms, and Consequences. Special Publication 82. Society for Sedimentary Geology, Tulsa, OK, pp. 1–5.

Hart, G.F., Palsey, M.A., Gregory, W.A., 1995. Particulate Organic Matter, Facies Models and Applications to Sequence Stratigraphy, in: Traverse, A. (Ed.), Sedimentation of Organic Particles. Cambridge University Press, pp. 337–390.

Hesselbo, S. P., Robinson, S. A., Surlyk, F., Piasecki, S., 2002. Terrestrial and marine extinction at the Triassic– Jurassic boundary synchronized with major carbon-cycle perturbations: a link to initiation of massive vol- canism? Geology 30, 251–254.

Hesselbo, S.P., Robinson, S.A., Surlyk, F., 2004. Sea-level changes and facies development across potential Triassic-Jurassic boundary horizons, SW Britain. Journal of Geological Society of London 161, 365–379.

Hillebrandt, A.V., Krystyn, L., Kürschner, W.M., Bonis, N.R., Ruhl, M., Richoz, S., Schobben, M. A. N., Urlichs, M., Bown, P.R., Kment, K., McRoberts, C.A., Simms, M., Tomãsových, A., 2013. The Global Stratotype Sections and Point (GSSP) for the base of the Jurassic System at Kuhjoch (Karwendel Mountains, Northern Calcareous Alps, Tyrol, Austria). Episodes 36, 162-198.

Katz, B.J., 2005. Controlling Factors on Source Rock Development — A Review of Productivity, Preservation and Sedimentation Rate. In: Harris, N.B. (Ed.), The deposition of organic-carbon-rich sediments: models, mechanisms and consequences. SEPM Special Publication, pp. 7–16

Korte, C., Hesselbo, S.P., Jenkins, H.C., Rickaby, R.E.M., Spotl, C., 2009. Palaeoenvironmental significance of carbon- and oxygen-isotope stratigraphy of marine Triassic–Jurassic boundary sections in SW Britain. Journal of the Geological Society 166, 431–445.

Kürschner, W.M., Bonis, N.R., Krystyn, L., 2007. Carbon-isotope stratigraphy and palynostratigraphy of the Triassic–Jurassic transition in the Tiefengrabensection Northern Calcareous Alps (Austria). Palaeogeography, Palaeoclimatology, Palaeoecology 244, 257–280.

Kürschner, W.M., Herngreen, G.F.W., 2010. Triassic palynology of central and northwestern Europe: a review of palynofloral diversity patterns and biostratigraphic subdivisions. Geological Society, London, Special Publications 334, 263-283.

Kürschner, W.M., Mander, L., McElwain, J. C. 2014. A gymnosperm affinity for *Ricciisporites tuberculatus* Lundblad: implications for vegetation and environmental reconstructions in the Late Triassic. Palaeobiodiversity and Palaeoenvironments 94, 295–305.

Lallier-Vergès, E., Tribovillard, N.P., Bertrand, P., 1995. Organic Matter Accumulation. Springer-Verlag, Berlin.

Lindström, S., 2016. Palynofloral patterns of terrestrial ecosystem change during the end-Triassic event – a review. Geological Magazine 153, 223-251.

Lindström, S., van De Schootbrugge, B., Dybkjær, K., Pedersen, G.K., Fiebig, J., Nielsen, H.N., Richoz, S., 2012. No causal link between terrestrial ecosystem change and methane release during the end-Triassic mass-extinction. Geology 40, 531–534.

Lindström, S., Erlström, M., Piasecki, S., Nielsen, L.H., Mathiesen, A., 2017a. Palynology and terrestrial ecosystem change of the Middle Triassic to lowermost Jurassic succession of the eastern Danish Basin. Review of Palaeobotany and Palynology 244, 65–95.

Lindström, S., van de Schootbrugge, B., Hansen, K.H., Pedersen, G.K., Alsen, P., Thibault, N., Dybkjær, K., Bjerrum, C.J., Nielsen, L.H., 2017b. A new correlation of Triassic–Jurassic boundary successions in NW Europe, Nevada and Peru, and the Central Atlantic Magmatic Province: A time-line for the end-Triassic mass extinction. Palaeogeography, Palaeoclimatology, Palaeoecology, 478, 80-102.

Lucas, S.G., Tanner, L.H., Donohoo-Hurley, L.L., Geissman, J.W., Kozur, H.W., Heckert, A.B., Weems, R.E., (2011). Position of the Triassic–Jurassic boundary and timing of the end-Triassic extinctions on land: Data from the Moenave Formation on the southern Colorado Plateau, USA. Palaeogeography, Palaeoclimatology, Palaeoecology 302, 194-205.

Marzoli, A., Bertrand, H., Knight, K.B., Cirilli, S., Vérati, C., Nomade, S., Martini, R., Youbi, N., Allenbach, K., Neuwerth, R., Buratti, N., Rapaille, C., Zaninetti, L., Bellieni, G., Renne, P.R., 2004. Synchrony of the Central Atlantic magmatic province and the Triassic–Jurassic boundary climatic and biotic crisis. Geology 32, 973-976.

Mascle, A., Vially, R., Deville, E., Biju-Duval, B., Roy, J.P., 1996. The petroleum evaluation of a tectonically complex area: The western margin of Southeast Basin (France). Marine and Petroleum Geology 13, 941 – 961.

Mattavelli, L., Chilingarian, G.V., Storer, D., 1969. Petrography and diagenesis of the Taormina formation, Gela Oil Field, Dicily (Italy). Sedimentary Geology 3, 59-86.

Meyer, K.M., Kump, L.R., 2008. Oceanic euxinia in Earth history: causes and consequences. Annual Review of Earth and Planetary Science 36, 251–288.6.

Michalik, J., Biroò, A., Lintnerová, O., Gotz, A.E., Ruckwied, K., 2010. Climatic change at the T/J boundary in the NW Tethyan Realm (Tatra Mts, Slovakia). Acta Geologica Polonica 60, 535-548.

Morbey, S.J., 1975. The palynostratigraphy of the Rhaetian stage, Upper Triassic in the Kendlbachgraben, Austria. Palaeontographica Abteluing B 152, 1–75.

Pacton, M., Fiet, N., Gorin, G.E., 2007. Bacterial activity and preservation of sedimentary organic matter: the role of exopolymeric substances. Geomicrobiology Journal 24, 571 – 581.

Pálfy, J., Zajzon, N., 2012. Environmental changes across the Triassic–Jurassic boundary and coeval volcanism inferred from elemental geochemistry and mineralogy in the Kendlbachgraben section (Northern Calcareous Alps, Austria). Earth Planet. Sci. Lett. 335–336, 121–134.

Pancost, R.D., Crawford, N., Magness, S., Turner, A., Jenkyns, H.C., Maxwell, J.R., 2004. Further evidence for the development of photic-zone euxinic conditions during Mesozoic oceanic anoxic events. Journal of the Geological Society 161, 353–364.

Parrish, J. T., 1993. Climate of the Supercontinent Pangea. Journal of Geology 10, 215-233.

Patacca, E., Scandone, P., Giunta, G., Liguori, V., 1979. Mesozoic paleotectonic evolution of the Ragusa zone (Southeastern Sicily). Geologica Romana 18, 331–369.

Perch-Nielsen K., 1989 Mesozoic calcareous nannofossils. In: Bolli, H.M., Saunders, J.B., Perch-Nielsen, K., (Eds.), Plankton Stratigraphy: Volume 1, Planktic Foraminifera, Calcareous Nannofossils and Calpionellids. Cambridge Earth Science Series, Cambridge University Press, pp. 329-426.

Perkins, R.B., Piper, D.Z., Mason, C.E., 2008. Trace-element budgets in the Ohio/Sunbury shales of Kentucky: constraints on ocean circulation and primary productivity in the Devonian–Mississippian Appalachian Basin. Palaeogeography Palaeoclimatology Palaeoecology 265, 14–29.

Robertson, A.H.F., Poisson, A., Akinci, O., 2003. Developments in research concerning Mesozoic Tertiary Tethys and neotectonics in the Isparta Angle, SW Turkey: Geological Journal 38, 195- 234.

Robinson, P.L., 1973. Palaeoclimatology and Continental Drift. In: Tarling, D.H., Runcorn, S.K. (Eds.), Implications of Continental Drift to the Earth Sciences, 1. Academic Press, London, pp. 451-476.

Rocchi, S., Langaretti, G., Ferrari, L., Carniolo, D., 1996, Evoluzione del magmatismo nel sottosuolo della Sicilia sud-orientale: dati sul chimismo dei clinopirosseni. Memorie della Società Geologica Italiana 51, 1101–1113.

Ruhl, M., Kürschner, W.M., Krystyn, L., 2009. Triassic-Jurassic organic carbon isotope stratigraphy of key sections in the western Tethys realm (Austria). Earth and Planetary Science Letters 281, 169-187.

Ruhl, M., Bonis, N.R., Reichart, G.J., Sinninghe, D.J.S., Kürschner, W.M., 2011. Atmospheric carbon injection linked to end-Triassic mass-extinction. Science 333, 430–434.

Ruiz-Martínez, V.C., Torsvik, T.H., van Hinsbergen, D.J.J., Gaina, C., 2012. Earth at 200 Ma: global palaeogeography refined from CAMP palaeomagnetic data. Earth and Planetary Science Letters 331-332, 67-79.

Satterley, A.K. 1996. The interpretation of cyclic successions of the Middle and Upper Triassic of the Northern and Southern Alps. Earth-Science Reviews 40, 181–207.

Schaller, M.F., Wright, J.D., Kent, D.V., 2011. Atmospheric pCO_2 perturbations associated with the Central Atlantic Magmatic Province. Science 331, 1404–1409.

Schoene, B., Guex, J., Bartolini, A., Schaltegger, U., Blackburn, T.J., 2010. Correlating the end-Triassic mass extinction and flood basalt volcanism at the 100 ka level. Geology 38, 387–390.

Schuurman, W.M.L., 1977. Aspects of Late Triassic palynology: 2. Palynology of the ‘Gre`s et Schiste a` Avicula contorta’ and ‘Argiles de Levallois’ (Rhaetian) of Northeastern France and Southern Luxemburg. Review of Palaeobotany and Palynology 23, 159–253.

Scotese, C.R., Schettino, A., 2017. Late Permian-Early Jurassic Paleogeography of Western Tethys and the World. In: Soto, J.I, Flinch, J.F., Tari, G., (Eds.), Permo-Triassic Salt Provinces of Europe, North Africa and the Atlantic Margins, Elsevier, pp. 57-95.

Sellwood, B.W., Valdes, P.J., 2007. Mesozoic climates. In: Williams, M., Haywood, A. M., Gregory, F.J., Schmidt, D.N., (Eds.). Deep-time Perspectives on Climate Change: Marrying the Signal from Computer Models and Biological Proxies. Micropalaeontological Society, Special Publications, pp. 201–224.

Steffen, D., Gorin, G.E., 1993. Palynofacies of the Upper Tithonian–Berriasian deep-sea carbonates in the Vocontian Trough (SE France). Bulletin des centres de recherches exploration-production Elf-Aquitaine 17, 235–247.

Sutherland, I.W., 2001. Biofilm exopolysaccharides: a strong and sticky framework. Microbiology 147, 3–9.

Trabucho-Alexandre, J., Hay, W.W., de Boer, P.L., 2012. Phanerozoic environments of black shale deposition and the Wilson Cycle. Solid Earth 3, 29–42.

Trincianti, E., Frixa, A., Sartorio, D., 2015. Palynology and Stratigraphic Characterization of Subsurface Sedimentary Successions in the Sicanian and Imerese Domains-Central Western Sicily. In: Bertini, A., Cirilli, S., Magri, D., Stephenson, M.H. (Eds.), Changing flora and vegetation through time in Italy. Review of Palaeobotany and Palynology 218, 48–66.

Tyson, R.V., 1995. Sedimentary Organic Matter - Organic Facies and Palynofacies. Chapman and Hall, London 1–615.

Tyson, R.V., 2001. Sedimentation rate, dilution, preservation and total organic carbon; some results of a modelling study. Org. Geochem. 32, 333–339.

Tyson, R.V., 2005. The "Productivity Versus Preservation" Controversy: Cause, Flaws and Resolution. In: Harris, N.B. (Ed.), The Deposition of Organic-carbon-rich Sediments: Models, Mechanisms, and Consequences. Special Publication 82. Society for Sedimentary Geology, Tulsa, OK, pp. 17–33.

Tyson, R.V., Pearson, T.H., 1991. Modern and Ancient Continental Shelf Anoxia: An Overview. In: Tyson, R.V., Pearson, T.H. (Eds.), Modern and Ancient Continental Shelf Anoxia. Geological Society of London. Special Publication 58, pp. 1–24.

Vajda, V., Calner, M., Ahlberg, A., 2013. Palynostratigraphy of dinosaur footprint-bearing deposits from the Triassic–Jurassic boundary interval of Sweden. GFF – A Scandinavian Journal of Earth Sciences 135, 120–130.

van de Schootbrugge, B., Quan, T.M., Lindström, S., Puttmann, W., Heunisch, C., Pross, J., Fiebig, J., Petschick, R., Röhling, H.G., Richoz, S., Rosenthal, Y., Falkowski, P.G., 2009. Floral changes across the Triassic/Jurassic boundary linked to flood basalt volcanism. Nature Geoscience 2, 589-594.

van der Zwan, C.J., 1990. Palynostratigraphy and palynofacies reconstruction of the Upper Jurassic to lowermost Cretaceous of the Draugen field, offshore mid Norway. Review of Palaeobotany and Palynology 62, 157–186.

Visscher, H. & Krystyn, L., 1978. Aspects of Late Triassic palynology. 4. A palynological assemblage from ammonoid-controlled late Karnian (Tuvalian) sediments of Sicily. Review of Palaeobotany and Palynology 26, 93–112.

Warrington, G., Cope, J.C.W., Ivimey-Cook, H.C., 2008. The St Audrie's Bay–Doniford Bay section, Somerset, England: updated proposal for a candidate Global Stratotype Section and Point for the base of the Hettangian Stage, and of the Jurassic System. International Subcommission on Jurassic Stratigraphy Newsletter 35, 2–66.

Whitaker, M.F., 1984. The Usage of Palynology in Definition of Troll Field Geology, Reduction of Uncertainties. Innovative reservoir geomodelling, 6th Offshore Northern Seas Conference and Exhibition, Stavanger, Norsk Petroleums-forening G6:1–44.

Whiteside, J.H., Olsen, P.E., Eglinton, T., Brookfield M.E., Sambrotto, R.N., 2010. Compound-specific carbon isotopes from Earth‘s largest flood basalt eruptions directly linked to the end-Triassic mass extinction. PNAS.1001706107, 1-5.

Wignall, P.B., 1991. Model for transgressive black shales? Geology 19, 167–170.

Wignall, P.B., Newton R., 2001. Black shales on the basin margin: a model based on examples from the Upper Jurassic of the Boulonnais, northern France. Sedimentary Geology 144, 335-356.

Wood, G.D., Gabriel, A.M., Lawson, J.C., 2002. Palynological Techniques - Processing and Microscopy. In: Jansonius, J., McGregor, D.C. (Eds.), 2nd editionPalynology: principles and applications. American Association of Stratigraphic Palynologists Foundation 1, 29–50.

Yaroshenko, O.P., 2007. Late Triassic palynological flora from Western Ciscaucasia. Palaeontological Journal 41, 1190- 1197.

Yellin-Dror, A., Grasso, M., Ben Avraham, Z., Tibor, G., 1997. The subsidence history of the northern Hyblean Plateau margin, southeastern Sicily. Tectonophysics 282, 277–289.

Figure captions

Fig. 1 Location of the study wells in the Late Triassic palaeogeographic scenario of the Hyblean Plateau (SE Sicily), at the initial drowing phase (modified from Cirilli et al., 2015); stars indicate the studied wells: Streppenosa 1 and Bimmisca 1, subject of this paper. Circles indicate the location of Pachino 4 well (Cirilli et al., 2015) and Polpo 1 (Frixa et al., 2000).

Fig. 2 Palaeoenvironmental restoration and facies distribution during the Late Triassic times of the Hyblean Plateau (not to scale). See the text for explanation.

Fig. 3 Scheme of the stratigraphic relationships of the Lower Mesozoic succession and age attribution according to various authors (not to scale). The vertical lines represent the stratigraphic interval covered by the two investigated wells: Bimmisca 1 (Bim1); Streppenosa 1 (Strep1).

Fig. 4 Range chart distribution of the terrestrial and marine palynomorphs across the Noto Formation and the Upper Streppenosa Member in the Streppenosa 1 well. Because samples are cuttings, the first downhole occurrences (FDOs) of palynomorphs have been used in constructing the range charts, in order to minimize the error introduced by caving.

Fig. 5 Range chart distribution of the terrestrial and marine palynomorphs across the Mila Member, Noto Formation and Upper Streppenosa Member in the Bimmisca 1 well. Because samples are cuttings, the first downhole occurrences (FDOs) of palynomorphs have been used in constructing the range charts, in order to minimize the error introduced by caving. Due to lost of circulation, the lowermost portion of Mila Member, from 3169 m (Total Depth) to 2908 m, lacks of samples.

Fig. 6 Streppenosa 1 well: lithostratigraphic log, lithofacies and palynofacies intervals (I - VI) defined on the basis of different organic debris percentages. PM1: vitrinite 1 and PM2: vitrinite 2; PM3: cutinite, PM4: inertinite; SP: sporomorphs (land spores and dispersed pollen grains); T: sporomorph tetrads; MC: marine components (dinoflagellate cysts, acritarchs and microforaminiferal linings); Botryoc: *Botryococcus* sp.; AOM: amorphous organic matter.

Fig. 7 Bimmisca 1 well: lithostratigraphic log, lithofacies and palynofacies intervals (I - V) defined on the basis of different organic debris percentages. PM1: vitrinite 1 and PM2: vitrinite 2; PM3: cutinite, PM4: inertinite; SP: sporomorphs (land spores and dispersed pollen grains); T: sporomorph tetrads; MC: marine components (dinoflagellate cysts, acritarchs and microforaminiferal linings); Botryoc: *Botryococcus* sp.; AOM: amorphous organic matter.

Plate I – Palynomorphs from Streppenosa 1 well: 1) *Baculatisporites* sp., Str 28, E.F. O46; 2) *Perinopollenites elatoides,* Str 28, E.F. J43/1; 3) *Deltoidospora mesozoica,* Str 12, E.F. P38/3; 4) *Dictyophyllidites mortonii,* Str 21, E.F. J42; 5) *Trachysporites fuscus,* Str 28, E.F. P48/1; 6) *Porcellispora longdonensis,* STR28, E.F. N29/3; 7) *Tsugaepollenites pseudomassulae,* Str 7, E.F. H36; 8) *Classopollis meyerianus,* Str 28, E.F. N41/3; 9) *Calamospora tener*, Str 29, E.F. F46; 10) *Carnisporites spiniger,* Str 28, E.F. S36/4; 11) *Acanthotriletes varius,* Str 28, E.F. W45/3; 12) *P.*

polymicroforatus, Str 28, E.F. N48/3; 13) *Araucariacites australis,* Str 28, E.F. F49/3; 14) *Ischyosporites variegatus,* Str 30, E.F. B38; 15) *Ischyosporites variegatus,* Str 28, E.F. J46/1; 16) *Triancoraesporites ancorae,* Str 28, E.F. R34; 17) *Schizosporis scissus,* Str 28, E.F. G39/4; 18) *Striatella seebergensis,* Str 45, E.F. N45/ 4; 19) *Classopollis torosus,* Str 45, E.F. U52/1; 20) *Classopollis torosus,* Str 45, E.F. Q24. Scale bar 10 µm.

Plate II. - Palynomorphs from Bimmisca 1 well: 1) *Dictyophyllidites mortonii,* Bim 16, E.F. P38; 2) *Trachysporites fuscus,* Bim 18, E.F. E51/4; 3) *Trachysporites fuscus,* Bim 17, E.F. T27/3; 4) *Deltoidospora mesozoica,* Bim 16, E.F. V44/4; 5) *Converrucosisporites* sp., Bim 25, E.F. Q34; 6) *P. polymicroforatus,* Bim 15, E.F. G49/3; 7) *Classopollis meyerianus,* Bim 16, E.F. G32; 8) *Kraeuselisporites* sp., Bim 16, E.F. N33/4; 9) *Paraklukisporites foraminis,* Bim 18, E.F. F45/1; 10) *Limbosporites lundbladiae,* Bim 17, E.F. V45; 11) *Verrucosisporites* sp., Bim 17, E.F. P40/1; 12) *Granulatisporites* sp., Bim 19, E.F. F44/2; 13) *Schizosporis scissus,* Bim 19, E.F. G35/3; 14) *Perinopollenites elatoides,* Bim 18, E.F. H50/1; 15) *Leptolepidites reissingeri,* Bim 18, E.F. J42/2; 16) *Porcellispora longdonensis,* Bim 16, E.F. M42/1; 17) *Porcellispora longdonensis,* Bim 16, E.F. E.F. N42/1; 18) *Ischyosporites variegatus,* Bim 1, E.F. E.F. R40/1; 19) *Retitriletes austroclavadites,* Bim 17, E.F. T50; 20) *Convolutispora klukiforma,* Bim 16, E.F. V39/2. Scale bar 10 µm.

Plate III Palynofacies from the studied interval of Streppenosa 1 well: 1) Interval I-Palynofacies A (Noto Formation), dominated by inertinite and low percentage of other palynomacerals (Str9); 2) Interval II-Palynofacies B (Noto Formation) from the shaly intervals, with moderate to high percentages of inertinite and vitrinite (Str11); 3) Interval III - Palynofacies C (Noto Formation) with low percentages of vitrinite 2, moderate inertinite and low AOM content from marly limestone (Str23); 4) Interval IV-Palynofacies D (include the Noto Formation and Upper Streppenosa Member boundary), with moderate to high amount of vitrinite, inertinite, sporomorphs and AOM (Str28); 5) Interval V - Palynofacies E, with abundant inertinite and less vitrinite and AOM (Str30); 6) Interval VI - Palynofacies F (Upper Streppenosa Member) with vitrinite, flakes of AOM and less inertinite at the base of the interval (Str36). Scale bar 200 µm.

Plate. IV Palynofacies from the studied interval of Streppenosa 1 well (1) and Bimmisca 1 well (2-6). 1) Streppenosa 1 well, Interval VI - Palynofacies F (Upper Streppenosa Member) with abundant AOM, inertinite and less pyrite (Str45); 2) Bimmisca 1 well, interval I - Palynofacies G (Mila Member of the Noto Formation) high content of vitrinite 1 and minor inertinite, moderate AOM from the microbial carbonates at the top of the interval; oil drops are visible (Bim37); 3) Interval II - Palynofacies H (Noto Formation), moderate to high content of inertinite, vitrinite and minor AOM (Bim26); 4) Interval III - Palynofacies I (Upper Streppenosa Member) abundant vitrinite, subordinate inertinite and flakes of AOM in the shaly intervals (Bim24); 5) Interval IV- Palynofacies L (Upper Streppenosa Member) dominated by inertinite with few others palynomacerals (e.g. vitrinite) (Bim14); 6) Interval V - Palynofacies M, shows an abrupt decrease in the total OM content mostly composed of inertinite (Bim1). Scale bar 200 µm.

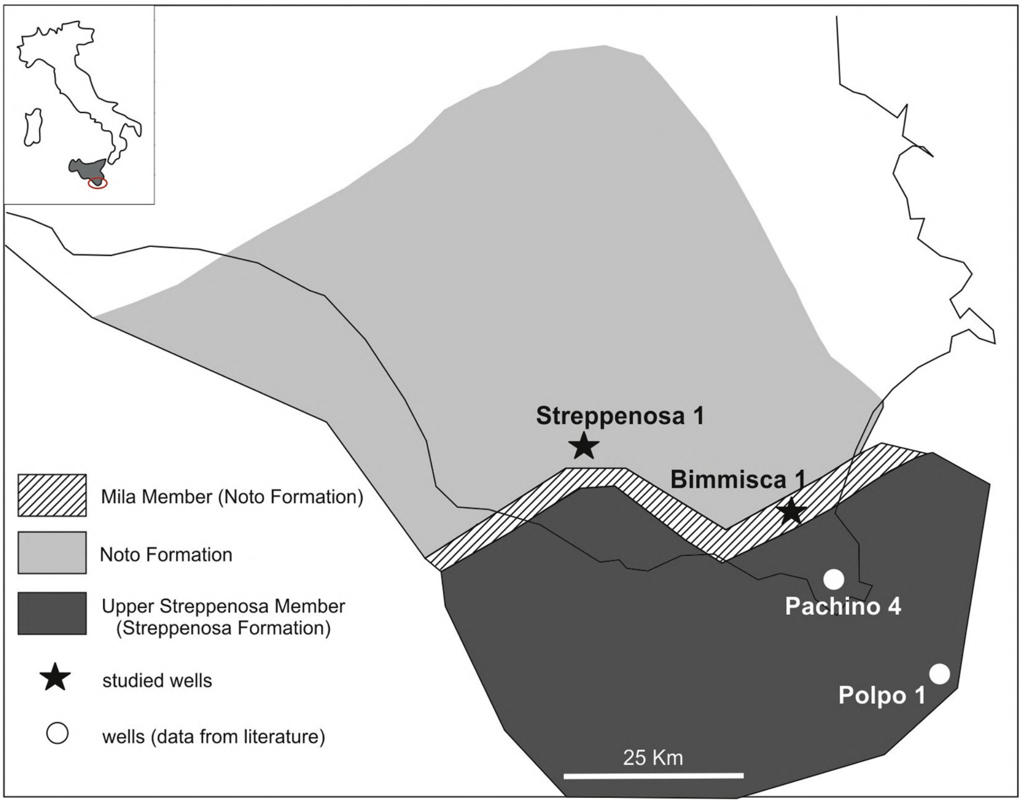
Streppenosa 1
Bimmisca 1
Pachino 4
Polpo 1
Mila Member (Noto Formation)
Noto Formation
Upper Streppenosa Member
(Streppenosa Formation)
studied wells
wells (data from literature)
25 Km

Fig. 1

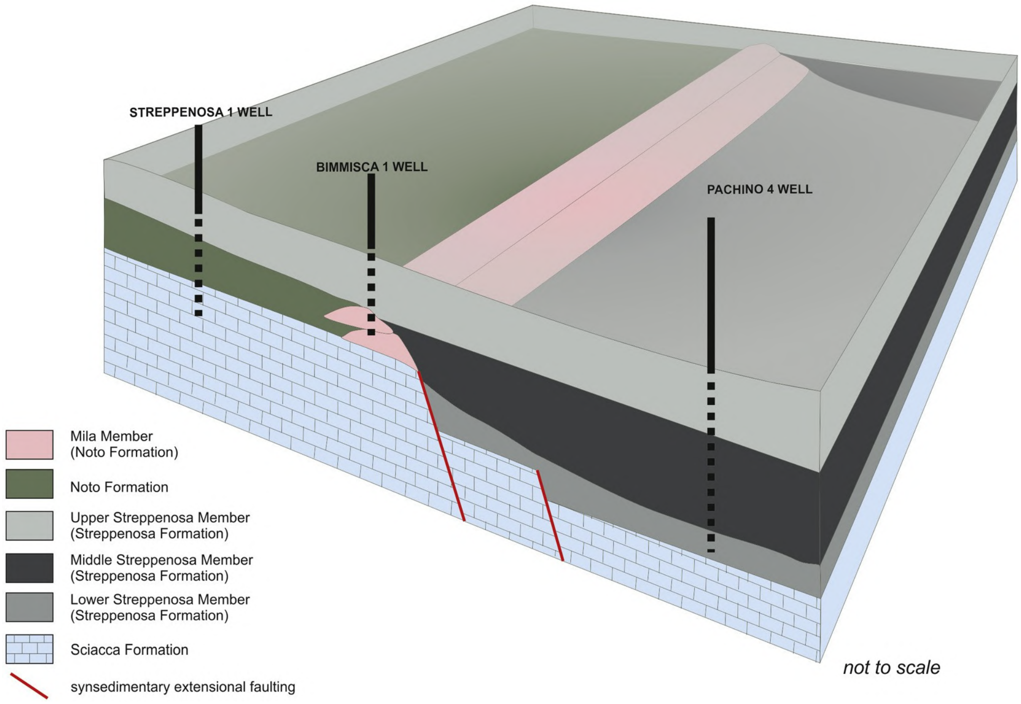
STREPPENOSA 1 WELL
BIMMISCA 1 WELL
PACHINO 4 WELL
Mila Member
(Noto Formation)
Noto Formation
Upper Streppenosa Member
(Streppenosa Formation)
Middle Streppenosa Member
(Streppenosa Formation)
Lower Streppenosa Member
(Streppenosa Formation)
Sciacca Formation
synsedimentary extensional faulting
not to scale

Fig. 2.

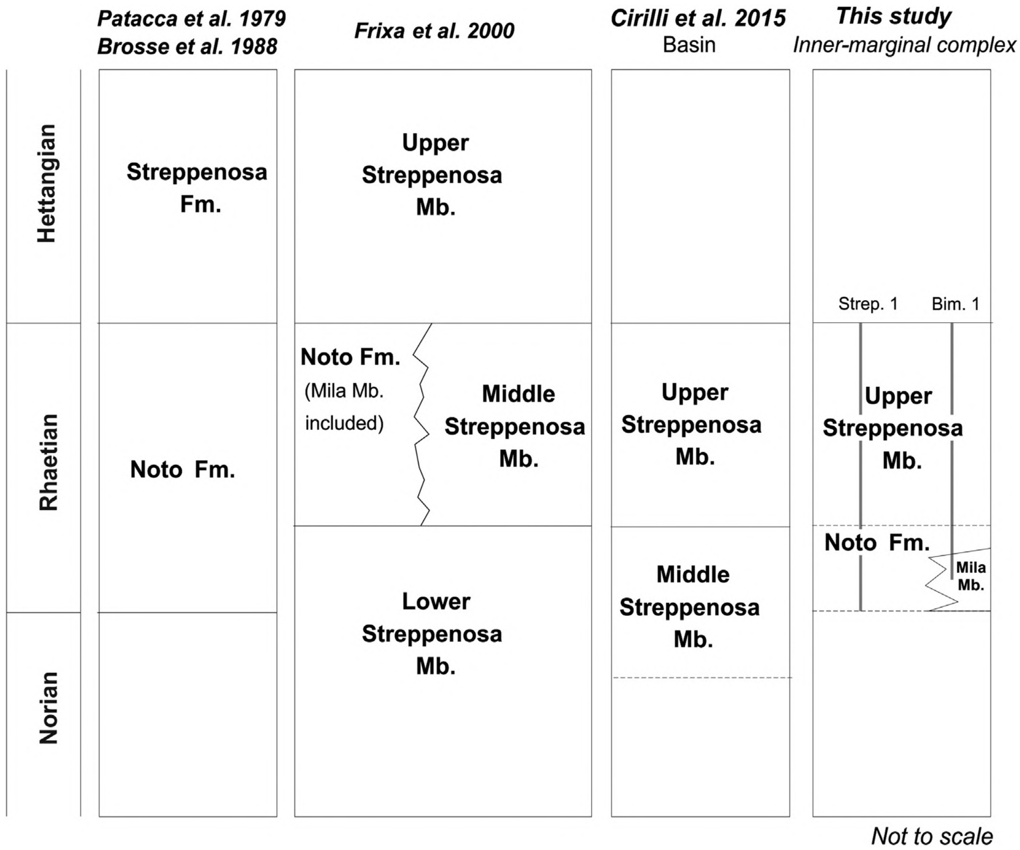
Patacca et al. 1979
Brosse et al. 1988
Frixa et al. 2000
Cirilli et al. 2015
Basin
This study
Inner-marginal complex
Hettangian
Rhaetian
Norian
Streppenosa Fm.
Noto Fm.
Upper Streppenosa Mb.
Noto Fm. (Mila Mb. included)
Middle Streppenosa Mb.
Lower Streppenosa Mb.
Upper Streppenosa Mb.
Middle Streppenosa Mb.
Strep. 1
Bim. 1
Upper Streppenosa Mb.
Noto Fm.
Mila Mb.
Not to scale

Fig. 3.

Fig. 4.

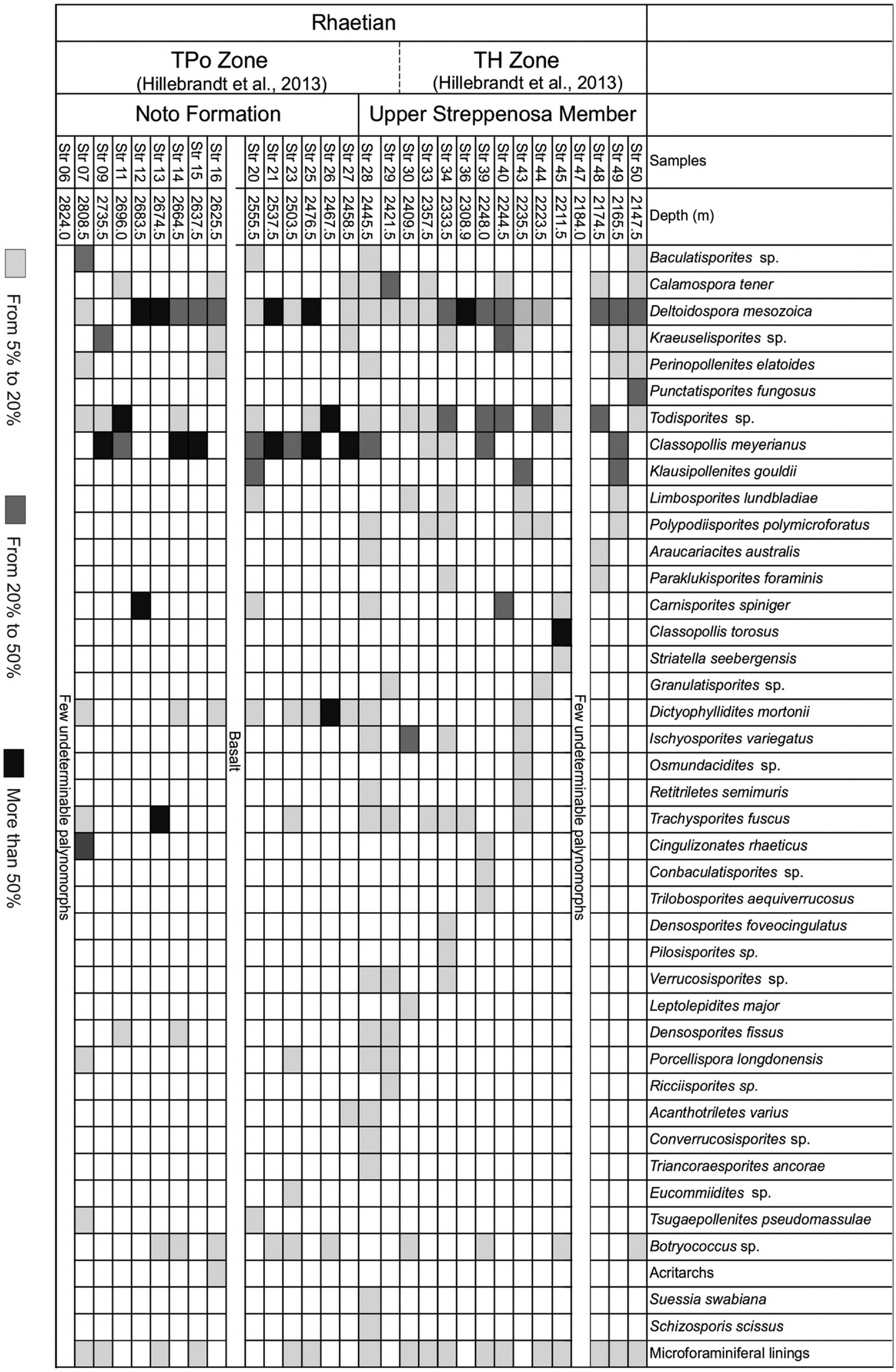

Rhaetian
TPo Zone
(Hillebrandt et al., 2013)
TH Zone
(Hillebrandt et al., 2013)
Noto Formation
Upper Streppenosa Member
Samples
Depth (m)
Str 06 2824.0
Str 07 2808.5
Str 09 2735.5
Str 11 2696.0
Str 12 2683.5
Str 13 2674.5
Str 14 2664.5
Str 15 2637.5
Str 16 2625.5
Str 20 2555.5
Str 21 2537.5
Str 23 2503.5
Str 25 2476.5
Str 26 2467.5
Str 27 2458.5
Str 28 2445.5
Str 29 2421.5
Str 30 2409.5
Str 33 2357.5
Str 34 2333.5
Str 36 2308.9
Str 39 2248.0
Str 40 2244.5
Str 43 2235.5
Str 44 2223.5
Str 45 2211.5
Str 47 2184.0
Str 48 2174.5
Str 49 2165.5
Str 50 2147.5
Few undeterminable palynomorphs
Basalt
Few undeterminable palynomorphs
Baculatisporites sp.
Calamospora tener
Deltoidospora mesozoica
Kraeuselisporites sp.
Perinopollenites elatoides
Punctatisporites fungosus
Todisporites sp.
Classopollis meyerianus
Klausipollenites gouldii
Limbosporites lundbladiae
Polypodiisporites polymicroforatus
Araucariacites australis
Paraklukisporites foraminis
Carnisporites spiniger
Classopollis torosus
Striatella seebergensis
Granulatisporites sp.
Dictyophyllidites mortonii
Ischyosporites variegatus
Osmundacidites sp.
Retitriletes semimuris
Trachysporites fuscus
Cingulizonates rhaeticus
Conbaculatisporites sp.
Trilobosporites aequiverrucosus
Densosporites foveocingulatus
Pilosisporites sp.
Verrucosisporites sp.
Leptolepidites major
Densosporites fissus
Porcellispora longdonensis
Ricciisporites sp.
Acanthotriletes varius
Converrucosisporites sp.
Triancoraesporites ancorae
Eucommiidites sp.
Tsugaepollenites pseudomassulae
Botryococcus sp.
Acritarchs
Suessia swabiana
Schizosporis scissus
Microforaminiferal linings
From 5% to 20%
From 20% to 50%
More than 50%

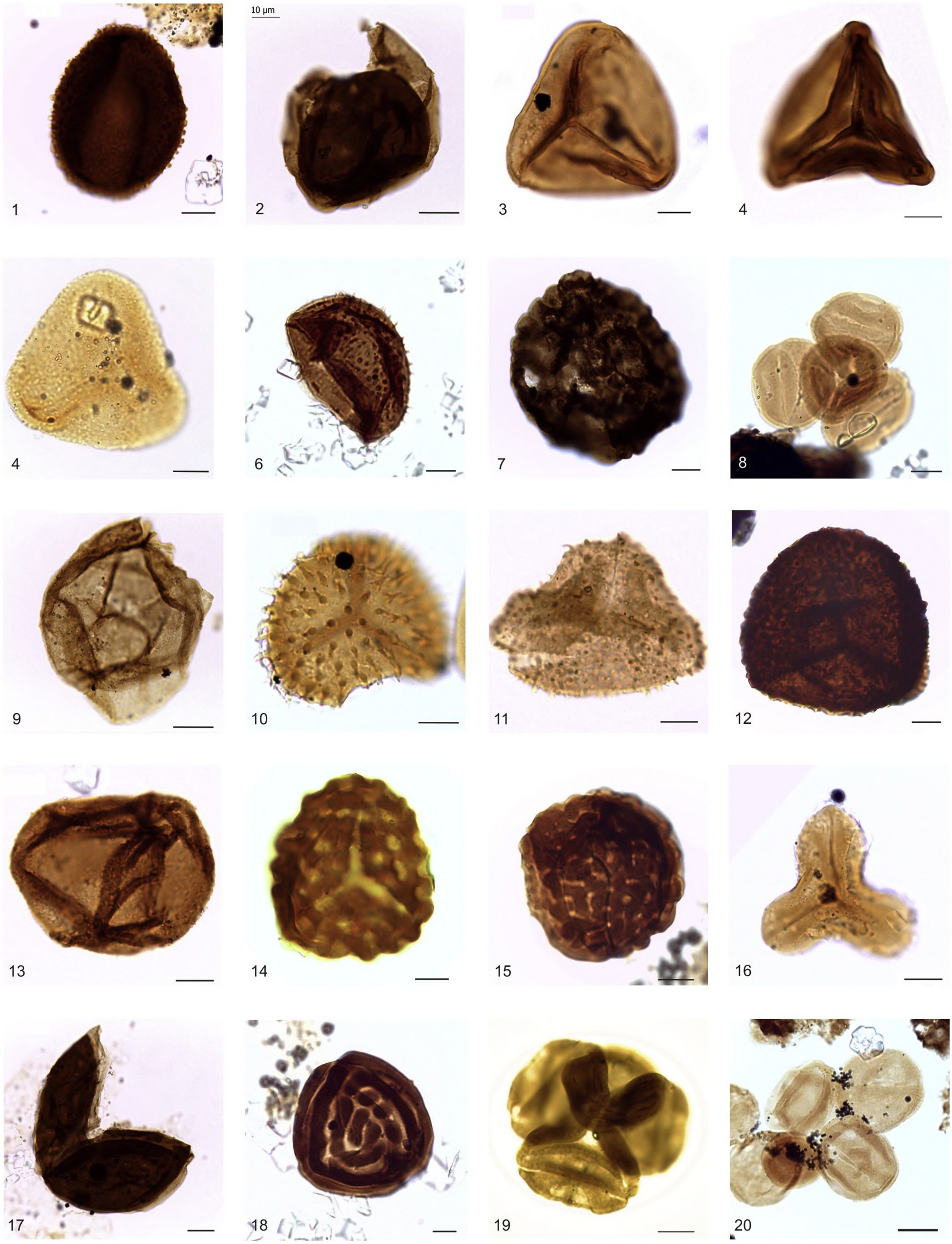

Plate 1

Fig. 5

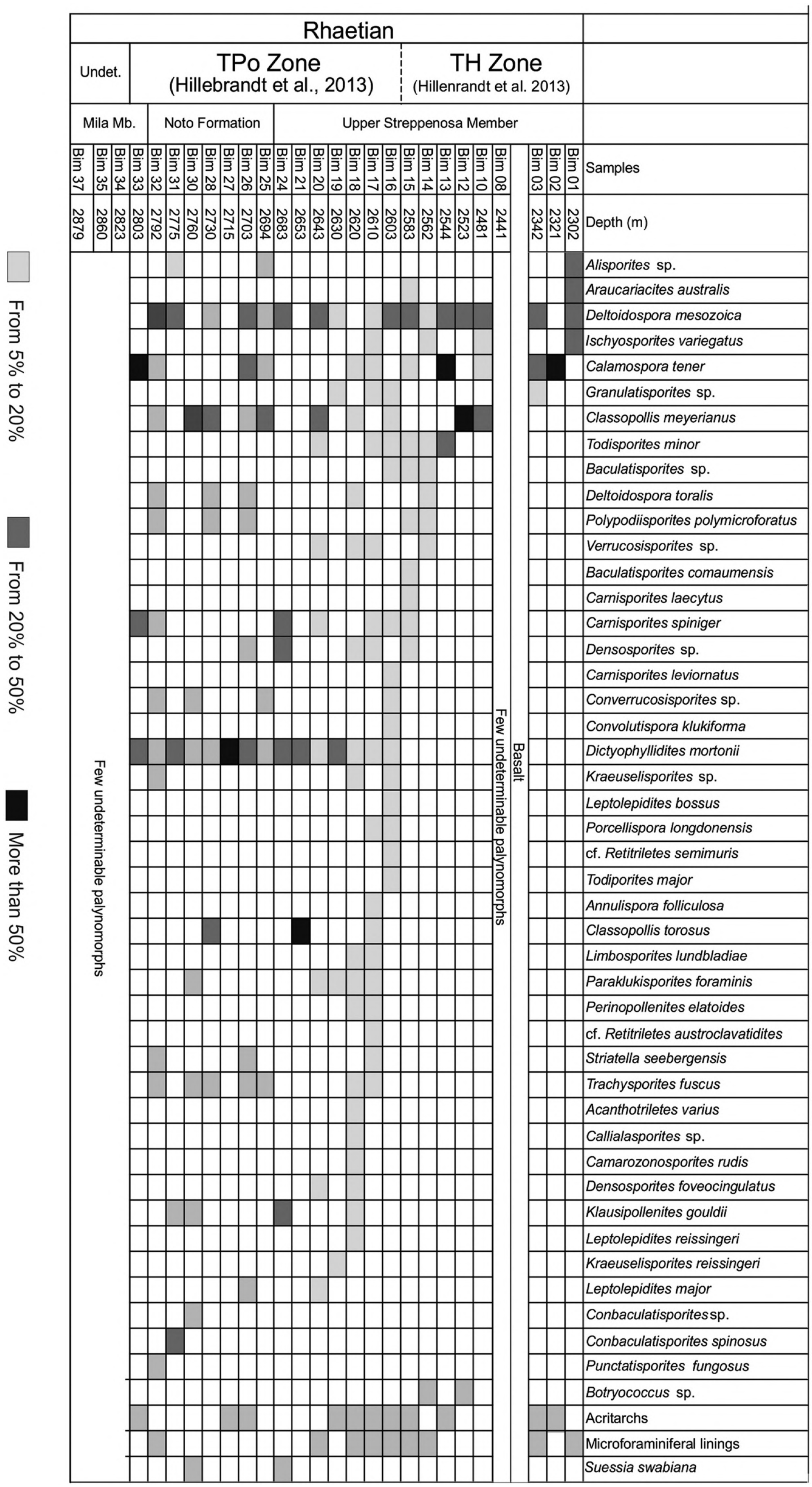

From 5% to 20%
From 20% to 50%
More than 50%
Rhaetian
Undet.
TPo Zone
(Hillebrandt et al., 2013)
TH Zone
(Hillenrandt et al. 2013)
Mila Mb.
Noto Formation
Upper Streppenosa Member
Samples
Depth (m)
Bim 37 2879
Bim 35 2860
Bim 34 2823
Bim 33 2803
Bim 32 2792
Bim 31 2775
Bim 30 2760
Bim 28 2730
Bim 27 2715
Bim 26 2703
Bim 25 2694
Bim 24 2683
Bim 21 2653
Bim 20 2643
Bim 19 2630
Bim 18 2620
Bim 17 2610
Bim 16 2603
Bim 15 2583
Bim 14 2562
Bim 13 2544
Bim 12 2523
Bim 10 2481
Bim 08 2441
Bim 03 2342
Bim 02 2321
Bim 01 2302
Few undeterminable palynomorphs
Few undeterminable palynomorphs
Basalt
Alisporites sp.
Araucariacites australis
Deltoidospora mesozoica
Ischyosporites variegatus
Calamospora tener
Granulatisporites sp.
Classopollis meyerianus
Todisporites minor
Baculatisporites sp.
Deltoidospora toralis
Polypodiisporites polymicroforatus
Verrucosisporites sp.
Baculatisporites comaumensis
Carnisporites laecytus
Carnisporites spiniger
Densosporites sp.
Carnisporites leviornatus
Converrucosisporites sp.
Convolutispora klukiforma
Dictyophyllidites mortonii
Kraeuselisporites sp.
Leptolepidites bossus
Porcellispora longdonensis
cf. Retitriletes semimuris
Todiporites major
Annulispora folliculosa
Classopollis torosus
Limbosporites lundbladiae
Paraklukisporites foraminis
Perinopollenites elatoides
cf. Retitriletes austroclavatidites
Striatella seebergensis
Trachysporites fuscus
Acanthotriletes varius
Callialasporites sp.
Camarozonosporites rudis
Densosporites foveocingulatus
Klausipollenites gouldii
Leptolepidites reissingeri
Kraeuselisporites reissingeri
Leptolepidites major
Conbaculatisporites sp.
Conbaculatisporites spinosus
Punctatisporites fungosus
Botryococcus sp.
Acritarchs
Microforaminiferal linings
Suessia swabiana

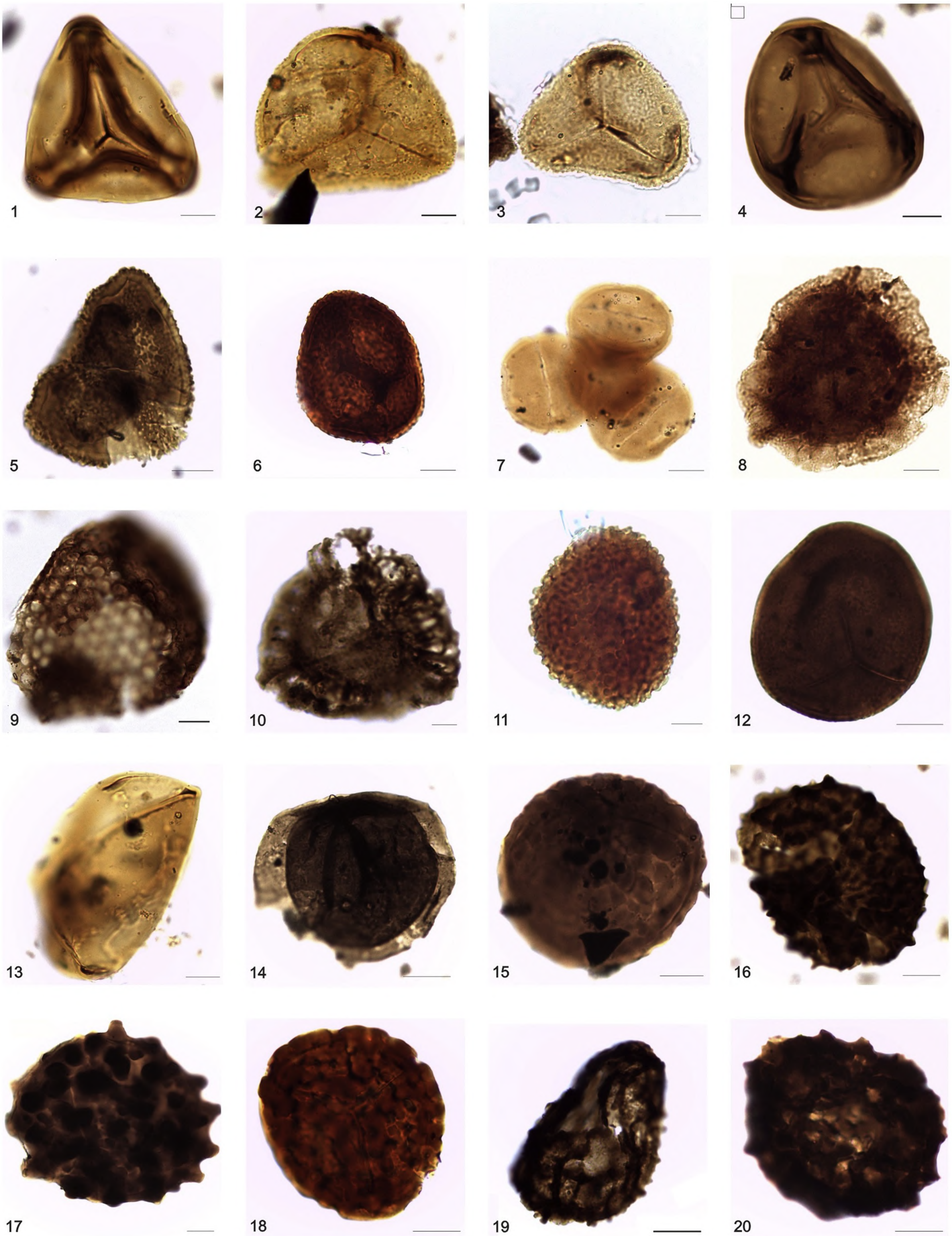

Plate 2

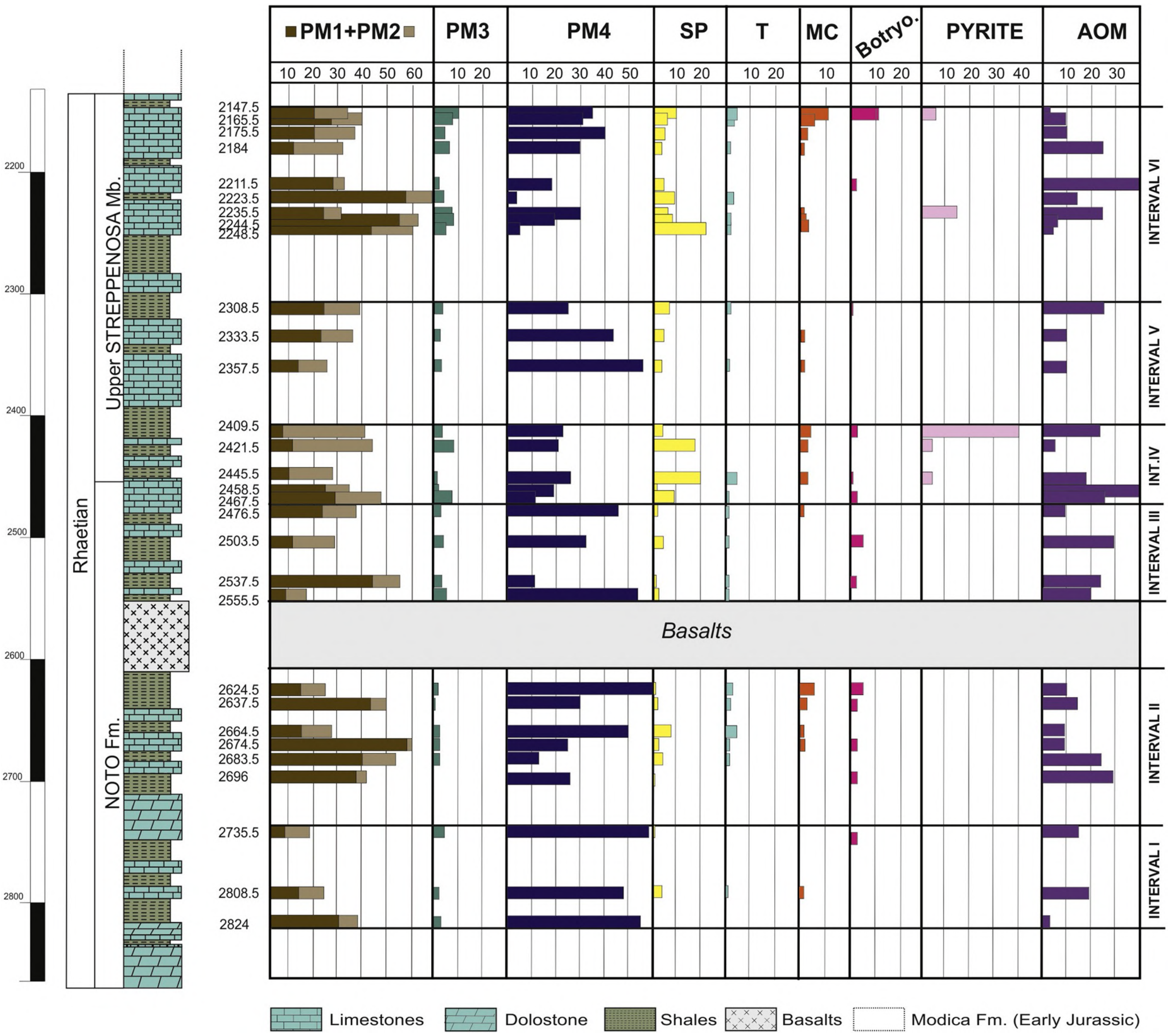

PM1+PM2
PM3
PM4
SP
T
MC
Botryo.
PYRITE
AOM
10 20 30 40 50 60
10 20
10 20 30 40 50
10 20
10 20
10
10 20
10 20 30 40
10 20 30
Rhaetian
Upper STREPPENOSA Mb.
NOTO Fm.
2200
2300
2400
2500
2600
2700
2800
2147.5
2165.5
2175.5
2184
2211.5
2223.5
2235.5
2244.5
2248.5
2308.5
2333.5
2357.5
2409.5
2421.5
2445.5
2458.5
2467.5
2476.5
2503.5
2537.5
2555.5
Basalts
2624.5
2637.5
2664.5
2674.5
2683.5
2696
2735.5
2808.5
2824
INTERVAL VI
INTERVAL V
INT.IV
INTERVAL III
INTERVAL II
INTERVAL I
Limestones
Dolostone
Shales
Basalts
Modica Fm. (Early Jurassic)

Fig. 6.

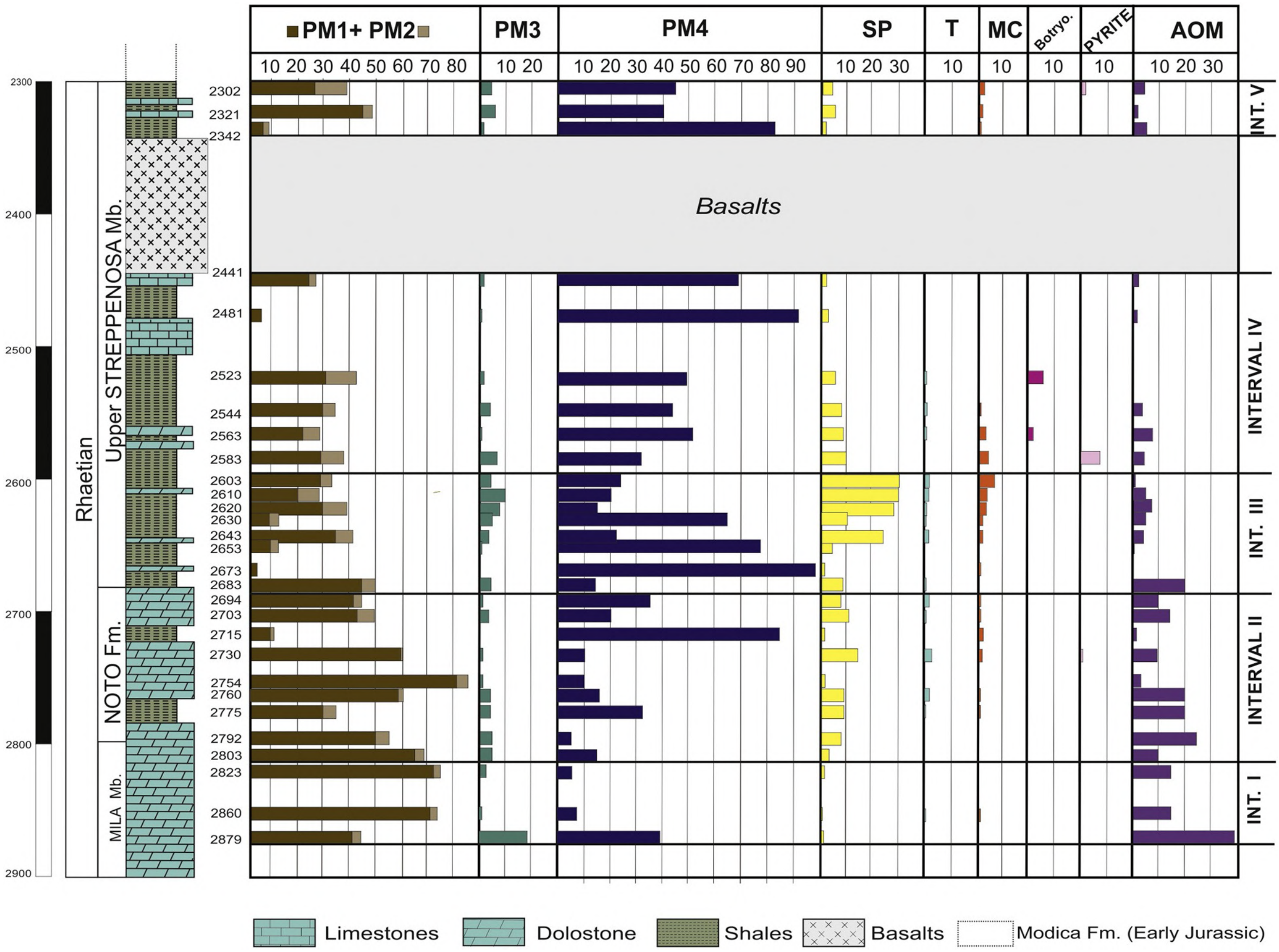

PM1+ PM2
PM3
PM4
SP
T
MC
Botryo.
PYRITE
AOM
Basalts
Rhaetian
Upper STREPPENOSA Mb.
NOTO Fm.
MILA Mb.
INT. V
INTERVAL IV
INT. III
INTERVAL II
INT. I
2300
2400
2500
2600
2700
2800
2900
2302
2321
2342
2441
2481
2523
2544
2563
2583
2603
2610
2620
2630
2643
2653
2673
2683
2694
2703
2715
2730
2754
2760
2775
2792
2803
2823
2860
2879
Limestones
Dolostone
Shales
Basalts
Modica Fm. (Early Jurassic)

Fig. 7.

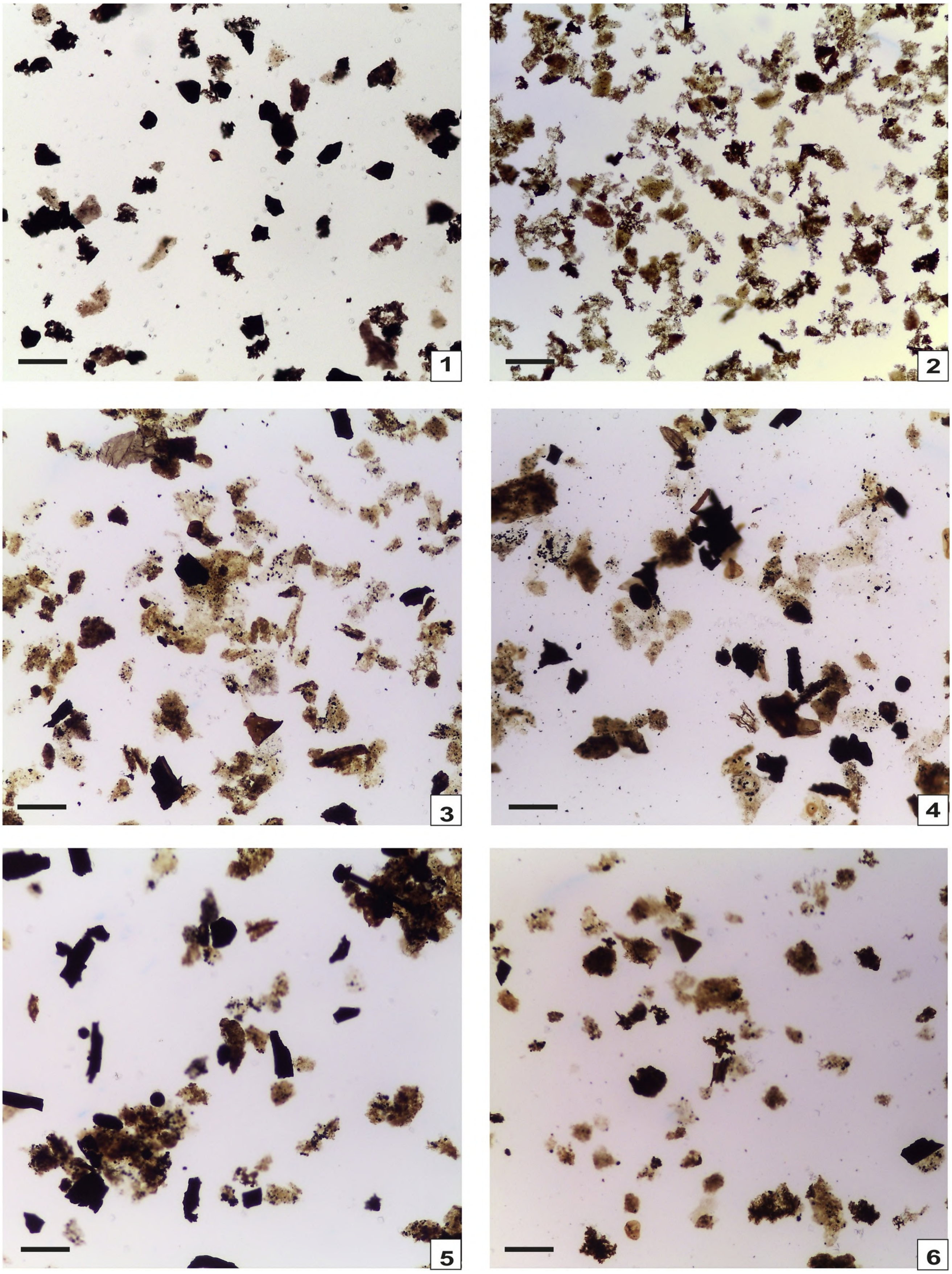

Plate 3

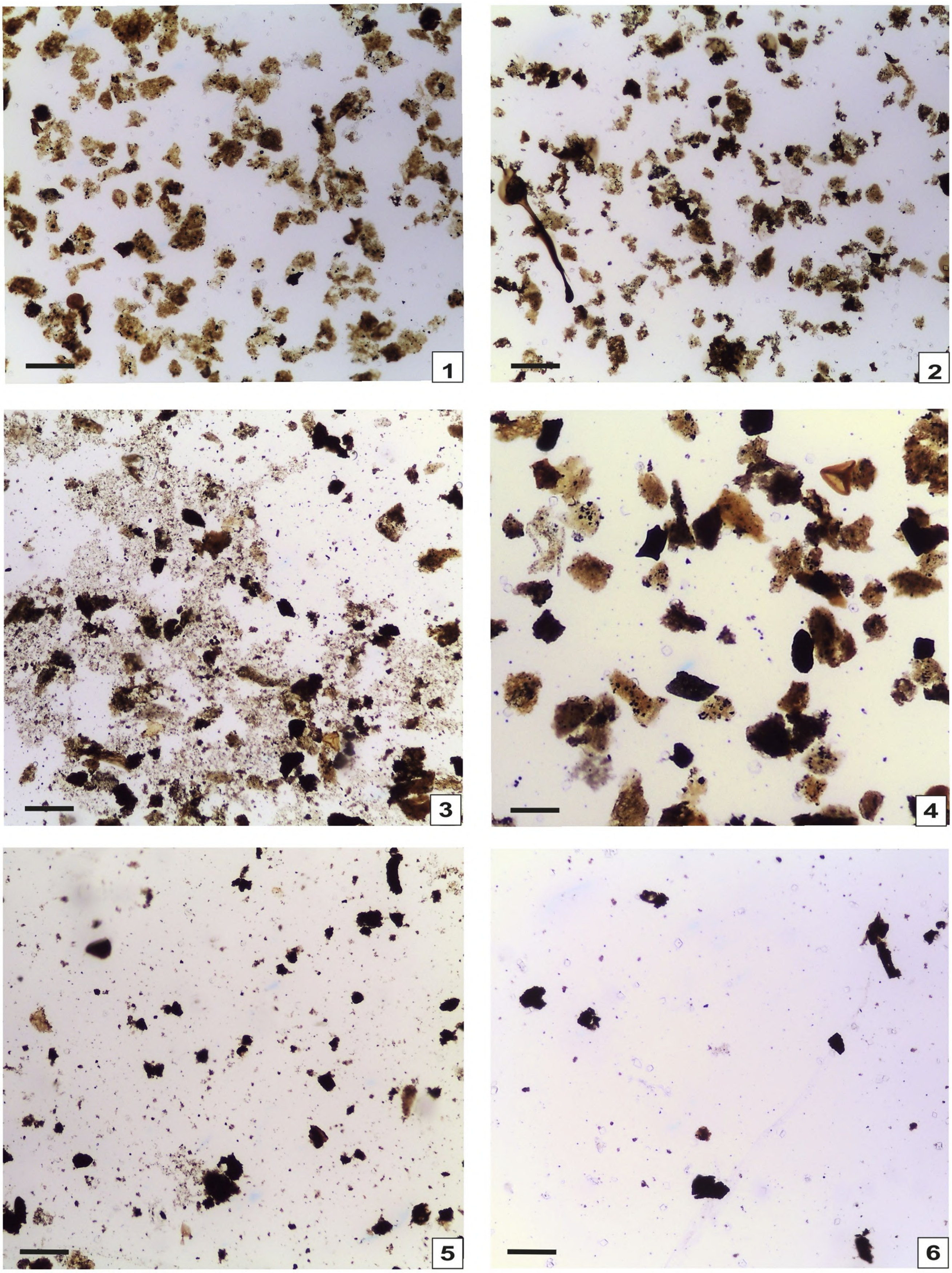

Plate 4